MONITORING INDUCED DENITRIFICATION DURING MANAGED AQUIFER RECHARGE IN AN INFILTRATION POND

Alba Grau-Martínez[a], Albert Folch[b,c], Clara Torrentó[a,d], Cristina Valhondo[c,e], Carme Barba[b,c], Cristina Domènech[a], Albert Soler[a], Neus Otero[a,f]

Abstract

Managed aquifer recharge (MAR) is a well-known technique for improving water quality and increasing groundwater resources. Denitrification (i.e. removal of nitrate) can be enhanced during MAR by coupling an artificial recharge pond with a permeable reactive layer (PRL). In this study, we examined the suitability of a multi-isotope approach for assessing the long-term effectiveness of enhancing denitrification in a PRL containing vegetal compost. Batch laboratory experiments confirmed that the PRL was still able to enhance denitrification two years after its installation in the infiltration pond. At the field scale, changes in redox indicators along a flow path and below the MAR-PRL system were monitored over 21 months during recharge and non-recharge periods. Results showed that the PRL was still releasing non-purgeable dissolved organic carbon five years after its installation. Nitrate concentration coupled with isotopic data collected from the piezometer network at the MAR system indicated that denitrification was occurring in the saturated zone immediately beneath the infiltration pond, where recharged water and native groundwater mix. Furthermore, longer operational periods of the MAR-PRL system increased denitrification extent. Multi-isotope analyses are therefore proved to be useful tools in identifying and quantifying denitrification in MAR-PRL systems.

Keywords: nitrate reduction, multi-isotope analysis, reactive layer, mixing zone, artificial recharge, field and laboratory experiments.

1. Introduction

Increasing water demands with growing world population and potential water shortages require flexible management strategies to replenish aquifers. The artificial recharge of groundwater, commonly known as managed aquifer recharge (MAR), is becoming increasingly important all over the world as a sustainable way of protecting the quality and quantity of groundwater supplies [Bouwer, 2002; Dillon, 2004; Sprenger et al., 2017]. Recharge ponds are one of the most commonly used approaches for MAR. This approach involves surface infiltration through spreading basins or ponds to introduce surface water into the subsurface environment [Bouwer, 2002; Miller et al., 2006].

Common sources of water for MAR in recharge ponds include wastewater effluents (after different stages of treatment) and effluent-receiving rivers [Díaz-Cruz and Barceló, 2008; Maeng et al., 2011], as well as river water and storm water runoff. These sources of water, mainly those from wastewater treatment plants (WWTPs), might contain high levels of ammonium (NH_4^+), whereas those resulting from agricultural activity might have high concentrations of nitrate (NO_3^-) [Schmidt et al., 2011]. Furthermore, oxic conditions promote ammonium nitrification, transforming it to nitrate.

The chemical composition of the infiltrating water in MAR changes due to a combination of physical and biogeochemical processes as the water passes from unsaturated to saturated zones, where it mixes with native groundwater. In some circumstances, these changes can lead to an overall improvement in groundwater quality [Bouwer, 2002; Fox et al., 2006]. Several studies have demonstrated that artificial recharge reduces the concentration of nutrients [Bekele et al., 2011], organic matter [Bekele et al., 2011; Vanderzalm et al., 2006], metals [Dillon et al., 2006; Bekele et al., 2011], pathogens [Dillon et al., 2006], organic contaminants [Dillon et al., 2006; Patterson et al., 2011] and pharmaceutically active compounds (PhACs) [Herber et al., 2004; Valhondo et al., 2014, 2015]. Massmann et al. [2006], investigated changes in redox conditions below an artificial recharge pond in Berlin, and found that the level of PhACs in groundwater was controlled by the transient hydraulic

and hydrochemical conditions during artificial recharge. Thus, to increase the quality of recharge water and groundwater, the infiltration pond can be coupled to a permeable reactive layer (PRL), an organic reactive layer at the bottom of the pond [Valhondo et al., 2014, 2015, 2016] that promotes diverse redox conditions along the recharge path to enhance the degradation of pollutants.

NO_3^- is one of the most abundant pollutants in groundwater [Li et al., 2010; Menció et al., 2016]. Denitrification, a microbe-mediated process in which NO_3^- is converted into dinitrogen gas (N_2), is the main naturally occurring process that decreases NO_3^- concentration in groundwater. Dilution and dispersion also decrease groundwater nitrate concentration, but in contrast to denitrification, they do not lead to mass reduction of the contaminant within an aquifer. Denitrification is carried out by bacteria that use NO_3^- as the terminal electron acceptor when dissolved oxygen (DO), which is energetically more favorable, is unavailable [Knowles, 1982]. Denitrification can be heterotrophic or autotrophic, depending on whether the substrate is organic or inorganic, respectively (Eq.1 and 2).

$$5CH_2O + 4NO_3^- + 4H^+ \rightarrow 2N_2 + 5CO_2 + 7H_2O \quad (1)$$

$$5FeS_2 + 14NO_3^- + 4H^+ \rightarrow 7N_2 + 10SO_4^{2-} + 5Fe^{2+} + 2H_2O \quad (2)$$

Denitrification can be enhanced in MAR-PRL pond systems, since adequate residence time and the presence of easily degradable organic carbon promote the activity of heterotrophic denitrifying bacteria. Recent laboratory studies [Grau-Martínez et al., 2017; Gibert et al., 2008] have suggested that low-cost carbon-releasing materials like organic compost, palm tree leaves and wood by-products could induce denitrification. Promoting denitrification by using a reactive layer in a recharge pond requires control mechanisms to test the efficacy of the implemented materials at the field scale.

Multi-isotope analysis, coupled with chemical data, is useful for identifying and even quantifying denitrification processes in aquifers [Mariotti et al., 1988; Aravena and Robertson, 1998; Pauwels et al., 2000, among others]. Denitrification affects the isotope composition of the residual nitrate, resulting in increased levels of the heavy isotopes ^{15}N and ^{18}O [Mariotti et al., 1988; Aravena and Robertson, 1998; Fukada et al., 2003; Kendall et al., 2007]. This

change in isotope composition, or isotope fractionation (ε), distinguishes denitrification at the field scale from other processes such as dilution, which can also decrease NO_3^- concentration, but without changing its isotopic value [Clark and Fritz, 1997; Kendall et al., 2007].

Isotopic studies coupled with chemical data are an effective tool to identify and describe denitrification [Aravena and Robertson, 1998; Pauwels et al., 1998, 2000, 2010; Kendall et al., 2007; Otero et al., 2009; among others]. Furthermore, multi-isotopic studies of the solutes involved in denitrification reactions, such as $\delta^{34}S$ and $\delta^{18}O$ of dissolved sulphate and $\delta^{13}C$ of dissolved inorganic carbon, can help determining whether denitrification is promoted by heterotrophic or autotrophic bacteria and identifying the occurrence of secondary processes such as SO_4^{2-} reduction [Mariotti et al., 1988]. Schmidt et al. [2011, 2012] used nitrate isotope ratios to demonstrate the occurrence of denitrification in the infiltrating water during its passage through the first meter of the soil beneath the base of a MAR pond in central coastal California.

In the present work, we monitored denitrification processes in a MAR-PRL system located at Sant Vicenç dels Horts, Barcelona, Spain [Valhondo et al., 2014, 2015, 2016, 2018], which has a layer of vegetal compost at the bottom of the infiltration pond. The aim of the present study is to test the usefulness of a combined isotope analysis and depth specific hydrochemical data to: (i) assess the long-term effectiveness of the reactive layer in promoting denitrification 5 years after its installation; (ii) identify the denitrification processes occurring at different aquifer depths and locations along the saturated zone below the infiltration pond (including the mixing zone between recharge and native groundwater). The methods tested here can be applied in other sites to assess the efficacy of MAR ponds coupled to reactive layer PRL in promoting denitrification.

2. Materials and methods

2.1. Study site description

106 The field site studied is located 15 km inland from the Mediterranean coast, in the lower valley
107 of the Llobregat Delta (Catalonia, NE Spain). This area is characterized by a Mediterranean
108 climate, with average annual precipitation around 590mm. Precipitation is scarce in winter and
109 summer (monthly average of 37mm) and more frequent during spring (monthly average of 41
110 mm) and especially autumn (monthly average 77mm). The aquifer consists of Quaternary
111 alluvial sediments, mainly coarse gravel and sand with small clay lenses [Iribar et al., 1997].
112 The minerals present include quartz, calcite and dolomite, and the solid phase fraction of
113 organic carbon is less than 0.002 (g_{OC}/g_{soil}) [Barbieri et al., 2011]. At this location, the aquifer
114 extends to a depth of 23 to 27 m underground [Valhondo et al., 2014] and is located between
115 5 and 10 m below the Llobregat river bed, the river and aquifer thus being hydraulically
116 disconnected [Vázquez-Suñé et al., 2007]. The regional groundwater flow direction is from
117 NNW to SSE [Quevauviller et al., 2009], with a natural hydraulic gradient of 2.3‰. Previous
118 pumping tests determined the hydraulic parameters to be 1.4×10^{4} m^2 day^{-1} for transmissivity
119 and 0.03 for storage coefficient [Barahona-Palomo et al., 2011].
120 Groundwater is artificially recharged by infiltrating water from the Llobregat River via a system
121 of pipes and ponds. The river water is collected approximately 2 Km upstream of the MAR
122 system (Molins de Rei inlet) and flows by gravity through a concrete pipe to a decantation
123 pond (≈4,000 m^2). By the time the river reaches the capture point, it has received treated water
124 from more than 50 wastewater treatment plants [Köck-Schulmeyer et al., 2011]. In the
125 decantation pond, the sediments are allowed to settle for approximately 2-4 days before the
126 water is transferred by a concrete pipe to an infiltration pond (≈5,000 m^2) (Fig. 1). The
127 infiltration rate in the infiltration pond ranges from 0.5 to 2 m d^{-1}, whereas insignificant water
128 infiltration occurs in the decantation pond [Valhondo et al., 2014]..

129 A reactive layer was installed at the bottom of the infiltration pond in 2011 to create favorable
130 conditions for the biodegradation of the contaminants present in the infiltration water. The
131 reactive layer (≈65 cm thick) consists of aquifer sand (49.5% in volume), vegetal compost from
132 gardens and scrap wood (49.5%), clay (≤1%) and iron oxide dust (≤0.1%). The components

were mixed on site with an excavator until homogeneity was visually evident. The layer was covered with approximately 5 cm of sand to prevent the woody material from floating away. The compost in the reactive layer was added to promote microbial growth and redox conditions by providing organic matter to the infiltration water. The sand was added to provide structural integrity to the layer and guarantee high hydraulic conductivity. Finally, iron oxides and clay, consisting mainly of illite (33 wt%), smectite (16 wt%) and chlorite (9 wt%), were present to provide extra sorption capacity for cationic and anionic contaminants [Valhondo et al., 2014].

The MAR pond undergoes two main operational periods: (1) recharge periods (RPs), with continuous flow from the river to the pond (infiltration water is mainly river water with less than 1.5% contribution from precipitation on average) and (2) non-recharge periods (NRPs), when the pond is dried for operational redevelopment and/or when the infiltration is stopped because the quality of the river water is low. During recharge periods, total saturation conditions are not obtained [Valhondo et al., 2015, 2016].

NRPs are implemented when the control parameters of the infiltration water are exceeded, such as when NH_4^+ concentrations are higher than 1.5 mg L^{-1}, electrical conductivity (EC) is higher than 2000 µS cm^{-1}, river turbidity is greater than 100 NTU and input water turbidity exceeds 25 NTU. NRPs are also implemented when the clogged layer needs to be removed or the upper layer of sand has to be cleaned. During NRPs, the groundwater table declines and the bottom of the pond is exposed to the atmosphere.

A piezometric network consisting of seven piezometers was installed around the recharge MAR system (Fig. 1). Piezometer P1 (screened from 6 to 24 m) is located upstream of the infiltration pond and was used to monitor background groundwater. P3 (screened from 5 to 23 m) is located upstream of the infiltration pond, between the decantation and infiltration ponds, while P8 is located in the middle of the infiltration pond and is composed of three piezometers screened at different depths (P8.1 from 13 to 15 m, P8.2 from 10 to 12 m and P8.3 from 7 to 9 m). P8.3 was used to evaluate the behavior of the infiltration water through the vadose zone,

159 while P8.1 was used to monitor the recharge at the deepest point of the saturated zone. P2
160 (completely screened from 6 to 24 m) and P5 (screened from 5 to 21 m) are situated
161 downstream, at the edge of the infiltration pond. Additionally, P9 (screened from 9 to 24 m)
162 and P10 (screened from 6 to 20 m) are located 190 m and 200 m downstream of the infiltration
163 pond, respectively. Therefore, all the monitoring points, except P1 (native groundwater) and
164 P8.3 (infiltration water just after crossing the vadose zone), represent different ratios of
165 recharge water to native groundwater in the aquifer at different travel times. Travel time of the
166 infiltration water from the pond to the piezometers is around 18 to 24 hours for P8.3, nearly 2
167 days for P2 and P5, 10 days for P10 and P8.1, and more than 20 days for P9 [Valhondo et al.,
168 2014; 2016]

169 **2.2. Sampling surveys**

170 To assess the long-term effectiveness of the PRL, four sampling campaigns were performed
171 using the seven piezometers (Fig. 1) to evaluate nitrate removal under different operational
172 conditions in June 2013, September 2013, July 2014 and March 2015. The monitored period
173 started 5 years after the installation of the PRL. The June 2013 and July 2014 campaigns
174 were performed during RPs, and the other two during NRPs. Figure 2 shows the distribution
175 along time of the operational periods and the sampling campaigns. The system was under
176 RPs for a total of 222 days in 2013 and 213 days in 2014. In 2015, before the March 2015
177 campaign, the system was under NRPs for almost four months, whereas only two months of
178 non-recharge had occurred before the September 2013 campaign.

179 Sampling was carried out using depth-specific samplers (bailers). Bailers are considered
180 suitable for measuring groundwater nitrate concentration [Lasagna and De Luca, 2016]. Each
181 piezometer was sampled at three different depths (Fig. 1), which were selected according to
182 the stratigraphic profiles. A layer with high transmissivity was identified in the middle depth of
183 all the piezometers. This layer is composed of polygenic gravel and large-sized gravel with
184 medium fine sandy matrix. Although some sampling protocols [ENSAT, 2012] do not deem it

necessary to purge piezometers in aquifers with high transmissivity such as that of Sant Vicenç dels Horts (1.4×10^4 m^2 day^{-1}), we still purged the piezometers prior to sampling by removing well water three times at each specific depth. During the four sampling campaigns, samples from the Llobregat River were also collected, sometimes more than once on the same day.

Physicochemical parameters (pH, temperature (T) and EC) were measured *in situ*, using a Multi 3410 multi-parameter (WTW, Weilheim, Germany). Samples for measuring major cations were filtered through 0.2-µm Millipore® filters, preserved by the addition of 1% HNO_3^- and stored in polyethylene bottles at 4ºC until analysis. Samples for the analysis of major anions (Cl^-, NO_3^-, NO_2^- and SO_4^{2-}) and isotope ratios ($\delta^{15}N_{NO3}$, $\delta^{18}O_{NO3}$, $\delta^{34}S_{SO4}$, $\delta^{18}O_{SO4}$ and $\delta^{13}C_{HCO3}$) were filtered through 0.2-µm Millipore® filters and stored in polyethylene bottles. Samples for measuring NO_3^- isotopes were kept frozen until analysis, while those for $\delta^{18}O_{H2O}$ and $\delta^{2}H_{H2O}$ measurements were collected in glass flasks and filtered through 0.45-µm Millipore® filters. For isotope analyses, samples were taken only from the middle depth of each piezometer. Samples for the analysis of non-purgeable dissolved organic carbon (NPDOC) were collected in muffled (450°C, 4.5 hours) glass bottles, filtered through 0.45-µm Millipore® filters, acidified to pH 3 with hydrochloric acid and stored at 4°C until analysis. To measure dissolved inorganic carbon (DIC), samples were collected in glass bottles, filtered through 0.45-µm Millipore® filters and analyzed within a day.

2.3. Laboratory experiments

Batch experiments were performed with material extracted in 2013 from the PRL of the MAR pond system. The substrate was used within a few hours after extraction without any pre-treatment. Experiments were performed in triplicate, using 20 g of the PRL material and 400 mL of groundwater from the Llobregat aquifer (from P2) spiked with 0.80 mM of NO_3^- to evaluate the denitrification potential of the vegetal compost. The experiments were run in sterilized 500-mL glass bottles previously purged with N_2 for 15 minutes in a glove box in an

211 argon atmosphere to minimize the O_2 level. Experimental oxygen partial pressure in the glove
212 box was maintained between 0.1 and 0.3% O_2 and continuously monitored using an oxygen
213 partial pressure detector (Sensotran, Gasvisor 6) with an accuracy of ± 0.1% O_2. Batch
214 experiments were manually shaken once a day and aqueous samples (5 mL) were collected
215 daily using sterilized syringes. A ratio of solution/solid material at 90% of the initial value was
216 maintained.

217 The experiments were performed to check the reactivity of the extracted material and also to
218 estimate the isotopic fractionation (Ɛ) of N and O.

219 The NO_3^- pseudo-first order degradation rate constants (k') were calculated using Eq. (3),
220 where C_0 and C_t are the initial NO_3^- concentration and the NO_3^- concentration at time t,
221 respectively.

222 $$C_t = C_0 e^{-k't} \quad (3)$$

223 Isotopic fractionation during denitrification can be expressed as a Rayleigh distillation process
224 Eq. (4), from which the isotopic fractionation factor (α) can be obtained [Mariotti et al., 1988;
225 Aravena and Robertson, 1998].

226 $$\ln\left(\frac{R_t}{R_0}\right) = (\alpha - 1) \ln\left(\frac{C_t}{C_0}\right) \quad (4)$$

227 where C_0 and C_t are the initial and residual NO_3^- concentration, respectively (mmol L^{-1}), and
228 R_o and R_t denote the ratios of heavy to light isotopes at the initial time and time t, respectively,
229 which are calculated according to Eq. (5).

230 $$R = \left[\left(\frac{\delta}{1000}\right) + 1\right] \quad (5)$$

231 Where δ is the isotopic composition of $\delta^{15}N$ and $\delta^{18}O$ (‰). The term (α -1) was calculated from
232 the slope of the regression line in the double-logarithmic plots $[\ln(R_t/R_0)]$ vs. $[\ln(C_t/C_0)]$,
233 according to Eq. (5), and converted into isotope fractionation (εN and εO) following Eq. (6).

$$\varepsilon = 1000 \text{ x } (\alpha - 1) \quad (6)$$

The Rayleigh equation applies to closed system conditions; therefore, isotopic fractionation is commonly calculated in laboratory experiments where conditions are wells constrained, no other sinks affect the NO_3^- pool and the concentration and isotopic composition of NO_3^- can be considered exclusively determined by NO_3^- reduction.

2.4. Analytical methods

Concentrations of major anions (Cl^-, NO_2^-, NO_3^-, and SO_4^{2-}) were determined by high performance liquid chromatography (HPLC) using a WATERS 515 HPLC pump, an IC-PAC anions column and a WATERS 432 detector. Cation concentrations were determined by inductively coupled plasma-optical emission spectrometry (ICP-OES, Perkin-Elmer Optima 3200 RL). NPDOC was measured by organic matter combustion using a MULTI N/C 3100 Analytik Jena carbon analyzer. DIC concentrations were analyzed by titration (METROHM 702 SM Titrino). Chemical analyses were conducted at the "Centres Científics i Tecnològics" of the University of Barcelona (CCiT-UB).

The $\delta^{15}N$ and $\delta^{18}O$ of dissolved NO_3^- were measured using a modified cadmium reduction method of McIlvin and Altabet [2005] and Ryabenko et al. [2009]. Briefly, NO_3^- was converted into nitrite through a spongy cadmium reduction and then to nitrous oxide using sodium azide in an acetic acid buffer. Simultaneous $\delta^{15}N$ and $\delta^{18}O$ analysis of the N_2O produced was carried out with a PreCon system (Thermo Scientific) coupled to a Finnigan MAT-253 Isotope Ratio Mass Spectrometer (IRMS, Thermo Scientific). For $\delta^{34}S$ and $\delta^{18}O$ analyses, dissolved SO_4^{2-} was precipitated as $BaSO_4$ by adding $BaCl_2$ after acidifying the sample with HCl and boiling it to prevent $BaCO_3$ precipitation, following standard methods [Dogramaci et al., 2001]. $\delta^{34}S$ was analyzed with a Carlo Erba elemental analyzer (EA)-Finnigan Delta C IRMS, while $\delta^{18}O$ was analyzed in duplicate with a ThermoQuest high temperature conversion EA (TC/EA) coupled in continuous flow with a Finnigan MAT Delta C IRMS. For $\delta^{13}C_{DIC}$ analysis, carbonates were

precipitated by adding a NaOH-$BaCl_2$ solution and isotope ratio was measured on a Gas-Bench II-MAT-253 IRMS (Thermo Scientific). δ^2H_{H2O} and $\delta^{18}O_{H2O}$ were analyzed by Wavelength-Scanned Cavity Ringdown Spectroscopy (WS-CRDS) using L2120-i Picarro®. Total C, total N, $\delta^{15}N$ and $\delta^{13}C$ from the PRL material were measured using Carbo Erba EA-Finnigan Delta C IRMS. Isotope ratios were calculated using both international and internal laboratory standards. Notation was expressed in terms of δ relative to the international standards (V-SMOW for $\delta^{18}O$ and δ^2H, atmospheric N_2 for $\delta^{15}N$, V-CDT for $\delta^{34}S$ and V-PDB for $\delta^{13}C$). The reproducibility of the samples was ±1‰ for the $\delta^{15}N$ of NO_3, ±1.5‰ for the $\delta^{18}O$ of NO_3^-, ±0.2‰ for the $\delta^{34}S$ of SO_4^{2-}, ±0.5‰ for the $\delta^{18}O$ of SO_4^{2-}, ±0.2‰ for the $\delta^{13}C$ of DIC, ±0.2‰ for the $\delta^{18}O$ of H_2O and ±1‰ for the δ^2H of H_2O. Samples for isotopic analyses were prepared at the "Mineralogia Aplicada i Geoquímica de Fluids" laboratory and analyzed at CCiT-UB, except water isotopes, which were analyzed at the University of Málaga.

3. Results and discussion

3.1. Laboratory experiments

Total N and C content as well as the $\delta^{15}N$ and $\delta^{13}C$ of the reactive layer material are shown in the Supplementary Material (Table S1). Results of the chemical and isotopic characterization of the batch experiments are detailed in the Supplementary Material (Table S2).

Complete NO_3^- reduction was achieved within eleven days in the batch experiments (Fig. 3), with a slight transient increase in NO_2^- concentration (up to 0.07 mM). Nitrate reduction in previous batch experiments performed with fresh commercial compost was accompanied by a significant initial release of NO_3^- (up to 2.5 mM) and transient NO_2^- production (up to 0.12 mM) [Grau-Martínez et al., 2017]. By comparison, the compost used in the present batch experiments, extracted from the PRL two years after its installation, did not release NO_3^- and produced a lower increase in NO_2^- concentration.

Denitrification in both sets of batch experiments followed pseudo-first-order kinetics and an

initial lag phase of 6-7 days with a lower degradation rate was observed. The observed k' values were 0.21±0.01 and 0.83±0.06 d^{-1} with the PRL material and 0.17±0.02 and 0.67±0.01 d^{-1} with the fresh compost for the lag and main phases, respectively. Although highly similar, degradation rates were slightly higher for the PRL material than for the fresh compost. These results demonstrated that the compost from the PRL still had denitrification potential two years after its installation.

The isotopic fractionations obtained were -10.4‰ for εN and -13.8‰ for εO, with a εN/εO ratio of 0.75 (Fig. 4a and 4b). The εN and εO values obtained in this study were similar to those from previous laboratory experiments using fresh commercial compost (εN= -10.8‰ and εO=-9.0‰ [Grau-Martínez et al., 2017]), also falling within the range of laboratory values for heterotrophic denitrification reported in the literature (from -8.6‰ to -16.2‰ for εN and from -4‰ to -13.8‰ for εO [Knöller et al., 2011; Carrey et al., 2013]).

The obtained C and N isotope fractionations associated with denitrification induced by the two-year-old PRL material enables a more accurate quantification of the enhanced reduction in NO_3^- levels in the aquifer.

3.2. Field study

3.2.1. Hydrochemical characterisation

Results of the chemical characterization of the field samples are detailed in the Supplementary Material (Table S3). For all the analyzed samples, pH values ranged between 6.98 and 7.60, HCO_3^- concentrations between 223 and 408 mg L^{-1} and EC from 991 to 1653 μS cm^{-1}. There were no significant differences in the concentrations of major cations between the piezometers among the four sampling campaigns.

Groundwater underneath the infiltration pond can be considered a mixture of recharge water and native groundwater. Samples clustered in the HCO_3-Cl-Ca-Na hydrochemical facies, with negligible differences among the sampling campaigns (Fig. S1).

3.2.2. Sources of groundwater recharge

Results of the isotopic characterization of the field samples are detailed in the Supplementary Material (Table S4). δ^2H and $\delta^{18}O$ values of the infiltration water (river water) and groundwater sampled during RPs (June 2013 and July 2014) mostly plotted along the Local Meteoric Water Line (LMWL) (Fig. 5). The LMWL was calculated with data from the Global Network of Isotopes in Precipitation (GNIP) obtained from stations 0818001 and 0818002 in Barcelona (IAEA/WMO, 2017). Isotope ratios are lower than the weighted mean long-term isotopic composition of precipitation in Barcelona (δ^2H= -31.16‰, $\delta^{18}O$= -5.3‰), but in agreement with the values obtained with the surface water of the Lower end of the Llobregat River [Otero et al., 2008] and samples from the Llobregat aquifer [Solà, 2009]. The results confirmed that river water is the main source of recharge in the aquifer and indicate that evaporation is not an important process in the pond and/or the unsaturated zone. Lastly, the range of δ^2H and $\delta^{18}O$ values showed that only one recharge flow system is involved in the aquifer recharge. Accordingly, Valhondo et al. [2015], using electrical conductivity and 1,1,2-trichloroethane content as tracers, estimated the contribution of the infiltration water on the monitoring points and showed that samples collected in P2, P5, P8.3 and P10 comprised primarily infiltrated water, whereas wells P8.2, P8.1 and P9 displayed a mixture of infiltration water and local groundwater (P1), although the concentrations were closer to the infiltration water composition.

3.3. Changes in redox sensitive indicators

The evolution of the concentration of NO_3^- and NPDOC in the saturated zone along the flow path, during both RPs and NRPs, is shown in Figure 6. The results of major anions (Cl^-, SO_4^{2-}, HCO_3^-) are shown in the Supplementary Material (Fig. S2).

For assessing the effect of MAR, the chemical composition of groundwater collected upstream

335 of the infiltration pond (P1, which represents native groundwater not affected by the recharge)
336 was compared to that of the piezometers affected by recharge water. The concentrations of
337 major anions in P1 samples remained almost constant with depth and time (Fig. S2). The
338 influence of river water is clearly observed in the piezometers located closer to the infiltration
339 pond (P8, P2 and P5) during RP and to a lesser extent during NRPs. Piezometers located
340 furthest from the infiltration pond (P9 and P10) are less influenced by river water chemistry.
341 Overall, no significant changes with depth were observed during both RP and NRPs.

342 NPDOC concentrations at the piezometers downstream of the infiltration pond generally
343 ranged between those for native groundwater and those for river water (Fig. 6) during both RP
344 and NRP, being generally lower during NRPs. Higher NPDOC concentrations were detected
345 in some samples (e.g. P2 in July 2014, P3 and P8 in September 2013, P8 in March 2015).
346 These results suggest that the reactive layer was still releasing NPDOC five years after
347 installation. Average higher NPDOC concentration was detected in September 2013 (two
348 months of non-recharge before sampling) than in March 2015 (four months of non-recharge
349 before sampling), indicating that the duration of recharge conditions had a significant effect.

350 NO_3^- concentration (measured as mg of NO_3^- L^{-1}) in native groundwater (P1) ranged from 4.2
351 to 9.8 mg L^{-1} with a median value of 5.6 (Table S3). Additional river water data show NO_3^-
352 contents between 4.5 and 17.4 mg L^{-1} (Table S5). It should be noted that NO_3^- and NH_4^+
353 concentrations vary considerably in rivers with effluents from WWTPs, even among samples
354 collected on the same day. During the RPs a significant decrease in NO_3^- concentration was
355 observed in the piezometers located close to the infiltration pond (P2 and P5), especially in
356 the June 2013 sampling, which showed complete NO_3^- reduction at some depths highlighting
357 the ability of the MAR-PRL system to enhance nitrate reduction (Fig. 6). During the July 2014
358 RP, a decrease in NO_3^- concentration was also observed downstream of the pond but to a
359 lesser extent. During NRPs, NO_3^- concentrations at the downstream piezometers were
360 generally within native groundwater and river water samples, although slightly lower NO_3^-
361 concentrations were seldom detected suggesting that NO_3^- reduction was maintained to some

extent.

Fe concentrations in samples downstream of the infiltration pond were generally lower than that in the native groundwater (P1) (Table S3). No significant variations between the sampling campaigns were observed (values ranged from 0.2 to 1.0 μM), except for an important increase at P5 during the June 2013 RP (up to 3.7 μM) probably arising from more reducing conditions occurring. The solubility of Fe(III)-oxyhydroxides, which usually affects Fe concentration in groundwater, increases under more reducing conditions, thereby increasing aqueous Fe concentration.

Overall, the observed changes in redox indicators suggested that the PRL installed in 2011 was still releasing organic matter and promoting reducing conditions to varying extents below the infiltration pond.

3.4. Denitrification during artificial recharge

Nitrate isotope composition was measured in a subset of these samples based on NO_3^- concentrations (Table S4). Figure 7 shows the $\delta^{15}N_{NO3}$ and $\delta^{18}O_{NO3}$ values of dissolved nitrate at the piezometers, as well as the isotope composition of the main potential sources of nitrate: nitrate fertilizers, ammonium fertilizers, soil nitrate and animal manure or sewage [Vitòria et al., 2004; Kendall et al., 2007; Xue et al., 2009]. The range of $\delta^{18}O$ of NO_3^- for ammonium fertilizers, soil nitrogen and manure/sewage plotted in Figure 7 (+1.93‰ to +3.13‰) was estimated according to Eq.7 [Anderson and Hooper, 1983; Kendall et al., 2007], where $\delta^{18}O_{H2O}$ corresponds to the range measured in Sant Vicenç dels Horts groundwater samples and $\delta^{18}O_{O2}$ to atmospheric O_2 (+23.5‰ [Horibe et al., 1973]).

$$\delta^{18}O_{NO3} = \frac{2}{3}(\delta^{18}O_{H2O}) + \frac{1}{3}(\delta^{18}O_{O2}) \quad (7)$$

Native groundwater (P1) showed $\delta^{15}N$ and $\delta^{18}O$ values ranging from +13.0 to +17.5‰ and from +2.8 to +9.7‰, respectively. The nitrate isotope ratios of the samples from the piezometers located downstream of the pond ranged from +9.5 to +26.7‰ (averaging

+18.4‰) for $\delta^{15}N$ and from +3.5 to +16.6‰ (averaging +9.5‰) for $\delta^{18}O$ (Table S4). All samples presented isotope ratios compatible with those for soil organic nitrogen and sewage/manure. The mixed groundwater samples showed a positive correlation (r^2=0.55) between $\delta^{15}N_{NO3}$ and $\delta^{18}O_{NO3}$ and were aligned following a εN/εO ratio of 1.5 (Fig. 7), which is consistent with denitrification [Kendall et al., 2007]. The εN/εO ratio reported in the literature for denitrification in groundwater ranges from 1.3 to 2.1 [Böttcher et al., 1990; Cey et al., 1999; Mengis et al., 1999; DeVito et al., 2000; Lehmann et al., 2003; Fukada et al., 2003].

Most samples collected during the RPs followed the denitrification trend, with higher $\delta^{15}N_{NO3}$ and $\delta^{18}O_{NO3}$ during the July 2014 sampling. During NRPs also a different behavior was observed in the two surveys, with lower isotopic values in March 2015 and high values in the September 2013 sampling. However, it should be noted that in both September 2013 and July 2014 samplings, high $\delta^{15}N$ and $\delta^{18}O$ values were also measured in river water. The high variability of NO_3^- contents in river water samples even on the same day (Table S5) could explain the particularly high isotope ratios measured in September 2013 and July 2014. Accordingly, Sine [2017] reported that NO_3^- isotopes values in a highly impacted river are not conservative, even when NO_3^- contents do not change. These authors studied the Grand River (south western Ontario, Canada), which receives high NO_3^- loading from point (urban WWTPs) and non-point sources (agricultural manure and fertilizer) and suggested that river metabolism influences rapid isotopic changes.

εN and εO values allow quantifying at field scale NO_3^- losses due to denitrification independently of dilution effects on NO_3^- concentrations [Mariotti et al., 1981; Böttcher et al., 1990; Fukada et al., 2003; Otero et al., 2009; Torrentó et al., 2011]. With the ε values obtained in laboratory experiments, the percentage of denitrification at the field scale can be calculated according to Eq. (8) using either εN or εO, or both.

$$\mathrm{DEN}\ (\%) = \left[1 - \frac{[NO_3]_{\mathrm{residual}}}{[NO_3]_{\mathrm{initial}}}\right] \times 100 = \left[1 - e^{\left(\frac{\delta_{(\mathrm{residual})} - \delta_{(\mathrm{initial})}}{\varepsilon}\right)}\right] \times 100 \qquad (8)$$

412 The extent of denitrification enhanced by the MAR-PRL system was estimated for each
413 sampling campaign. The isotope composition of the native groundwater (P1) for each
414 campaign was used as the initial value, and the ε values were obtained from the batch
415 experiments with the two-year-old PRL material (-10.4‰ for εN and -13.8‰ for εO, with an
416 εN/εO ratio of 0.75) (Fig. 8).

417 This approximation shows that during both RPs, the NO_3^- reduction percentage was similar
418 with a maximum value around 30% - 40%. Complete denitrification at some depths of P2 and
419 P5 was observed in samples collected in June 2013 (Fig. 6), but isotopic values were not
420 determined due to the low NO_3^- concentration. Denitrification was enhanced in the
421 piezometers located closer to the infiltration pond (P2). In all campaigns, the isotope
422 composition of P8.2 was very similar to that of P1, indicating that denitrification was not
423 occurring. Since isotopes in samples at different depths were not determined, the cause of
424 variations in NO_3^- concentration along depth at P8 could be either due to denitrification or other
425 process (e.g., mixing). Comparing the two RP sampling campaigns, the June 2013 samples
426 presented a slightly higher level of denitrification, most probably because the system was
427 under almost continuous operation since January 2012 (except for 30 days in August 2012,
428 24 days in February-March 2013 and 5 days in April 2013). The MAR system was stopped
429 from 22nd June to 1st July, 10 days before the July 2014 sampling campaign. The longer
430 operational period before the June 2013 campaign could have induced a well-developed
431 denitrifying microbial community, with the bacteria being more concentrated in the areas
432 receiving more recharge water, such as P2 and P5. Li et al. [2013], simulating the infiltration
433 zone of a MAR system, showed that microbial communities reached stability after 3-4 months
434 of operation.

435 During NRPs, the percentage of denitrification was very low (<20%) in all the samples, except
436 those from P2 (30-60%), which was one of the piezometers most affected by recharge water
437 [Valhondo et al., 2014] (Fig. 8). All the samples collected in March 2015, including P2, showed
438 the lowest percentage of denitrification among all the sampling campaigns. The September

2013 campaign was performed after a year of almost continuous recharge (Fig. 2) followed by less than two months of non-recharge, whereas the March 2015 campaign was undertaken after almost four months of non-recharge. Differences in the percentage of denitrification among the P2 samples collected from both NRPs indicate that the bacteria grow during RPs were still denitrifying even when the MAR pond was under non-recharge, but became less active with time in the absence of a carbon source [Rodríguez-Escales et al., 2016a; 2016b].

Results indicate that time of operation is a key issue to enhance denitrification in the MAR-PRL system. However, in practical terms it is difficult to accomplish due to day by day management issues (low quality river water, maintenance, etc.). In this regard, chaotic advection could be a good technology to keep high denitrification rates as well as other pollutant degradation in both RPs and NRPs as stated in Rodríguez-Escales et al. [2017].

3.5. Additional isotope data

On the one hand, the redox conditions induced in a MAR-PRL system determine the degradation of different contaminants. In the case of mixtures of emerging organic contaminants, for example, increasing the variability of redox conditions is crucial since the individual degradation of these compounds depends on specific redox conditions [e.g. Barbieri et al., 2011; Liu et al., 2013]. Characterizing the redox conditions achieved in the studied MAR-PRL system is thus critical.

Monitoring the redox sensitive indicators and the nitrate isotope data suggested that the organic matter released by the PRL was promoting reducing conditions to varying extents, at least to nitrate reduction conditions, and probably iron reductions conditions occasionally in P5. The isotope composition of SO_4^{2-} ($\delta^{34}S_{SO4}$ and $\delta^{18}O_{SO4}$) was analyzed to assess the occurrence of sulfate-reducing conditions. Sulfate reduction should produce a decrease in the SO_4^{2-} concentration an increase in the $\delta^{34}S_{SO4}$ values of the dissolved SO_4^{2-}. The isotope composition of the dissolved SO_4^{2-} in mixed groundwater samples was only analyzed for the June 2013 and September 2013 campaigns. Values ranged from +6.7 to +10.6‰ for $\delta^{34}S$ and

from +9.0 to +11.1‰ for $\delta^{18}O$ (Fig. 9). Similar values were obtained for the river water and native groundwater samples. Most of the mixed groundwater samples gave values within the range obtained for sewage [Otero et al., 2008] (Fig. 9), indicating that the vast majority of SO_4^{2-} came from sewage, which is consistent with the conclusions drawn from the NO_3^- isotope results regarding potential NO_3^- sources.

The narrow range of the $\delta^{34}S_{SO4}$ and $\delta^{18}O_{SO4}$ values obtained suggests a lack of SO_4^{2-} reduction. It can thus be concluded that the NPDOC released by the reactive layer produces variable redox conditions in the saturated zone along the flow path, leading mainly to the reduction of NO_3^-, as well as iron under certain conditions, but not of SO_4^{2-}. Results indicate that time of operation is a key issue to modify redox conditions as well as pollutant degradation in the MAR-PRL system.

On the other hand, the isotopic composition of dissolved inorganic carbon $\delta^{13}C_{HCO3}$ can provide information about the denitrification reaction [Aravena and Robertson, 1998]. However, in the studied site, due to the aquifer lithology, groundwater contained high concentrations of bicarbonate (median value of 325±25 mg L^{-1} in P1 for the four sampling campaigns) that could buffer any change in the $\delta^{13}C_{HCO3}$ isotope ratio linked to denitrification. The $\delta^{13}C_{HCO3}$ values in P1 samples (native groundwater) averaged -13.2±1‰, which is in agreement with the known range of $\delta^{13}C_{HCO3}$ for groundwater (-16‰ to -11‰ [Vogel and Ehhalt, 1963]). Mixed groundwater samples displayed $\delta^{13}C_{HCO3}$ values close to that of P1 samples (between -13.8 and -12.0‰, with a median value of -12.7‰), except three samples collected in the June 2013 campaign (RP) (that had values ranging from -11.1 to -9.9‰) (Fig. 10). As expected, the role of organic matter oxidation in the observed denitrification processes was not evident from the $\delta^{13}C_{HCO3}$ data due to the buffering effect of the bicarbonate.

4. Conclusions

We evaluated the feasibility of a multi-isotope approach for assessing the efficacy of the MAR-

PRL system of Sant Vicenç dels Horts in promoting denitrification in the groundwater below the infiltration pond. Similarities in the hydrochemical data (except for NO_3^- contents, which decreased during recharge periods in mixed groundwater) of river water, native groundwater and mixed groundwater demonstrated a unique recharge flow system. Changes in the redox indicators with depth and along the flow path during recharge and non-recharge periods confirmed that the reactive layer was still releasing NPDOC five years after installation. NO_3^- concentrations decreased during recharge periods especially in the piezometers closest to the infiltration pond, while aqueous Fe concentrations increased in the piezometers with lower NO_3^- concentrations, however, SO_4^{2-} reduction was not observed.

Isotope data revealed that denitrification mainly occurred in the area under the infiltration pond. The piezometers closest to the MAR-PRL, P2 and P5, showed higher levels of denitrification than the other piezometers. Importantly, denitrification was enhanced by a more continuous recharge of the MAR-PRL system, probably because microbial communities become stable after 3-4 months of continuous operation. Although a more detailed field sampling survey is needed to determine the real extent of denitrification at the field scale, the results of this study show the usefulness of a multi-isotope approach in identifying denitrification in MAR-PRL systems.

Acknowledgements

This study was funded by the projects REMEDIATION [ref. CGL2014-57215-C4-1-R] and ISOTEC [CGL2017-87216-C4-1-R], financed by the Spanish Ministry of Economy AEI/FEDER, EU, the project MAG [Catalan Government, ref. 2014SGR-1456] and the European Union projects WADIS-MAR [European Commission, ref. ENPI/2011/280-008] and MARSOL [European Commission, FP7-ENV-2013-WATER-INNO-DEMO]. We thank the editor and three anonymous reviewers for comments that improved the quality of the manuscript.

515 **References**

516 Anderson, K.K., Hooper, A.B., (1983). O_2 and H_2O are each the source of O in NO_2 produced
517 from NH_3 by Nitrosomas ^{15}N-NMR evidence. FEBS Lett. 64, 236-240.

518 Aravena, R., Robertson, W.D., (1998). Use of multiple isotope tracers to evaluate
519 denitrification in ground water: Study of nitrate from a large-flux septic system plume. Ground
520 Water 36, 975-982.

521 Barahona-Palomo, M., Barbieri, M., Fernàndez-Garcia, D., Pedretti, D., Sanchez-Vila, X.,
522 Valhondo, C., Queralt, E., Massana, J., Hernández, M., Tobella, J., (2011). Caracterització
523 del Sistema de Recàrrega de Sant Vicenç dels Horts: Projecte RASA, Informe Fase 2,
524 Barcelona: CUADLL.

525 Barbieri, M., Carrera, J., Sanchez-Vila, X., Ayora, C., Cama, J., Köck-Schulmeyer, M., López
526 de Alda, M., Barceló, D., Tobella Brunet, J., Hernández García, M., (2011). Microcosm
527 experiments to control anaerobic redox conditions when studying the fate of organic
528 micropollutants in aquifer material. J. Contam. Hydrol. 126 (3-4): 330-345.

529 Bekele, E., Toze, S., Patterson, B., Higginson, S., (2011). Managed aquifer recharge of
530 treated wastewater: water quality changes resulting from infiltration through the vadose zone.
531 Water Res. 45 (17), 5764-5772.

532 Böttcher, J., Strebel, O., Voerkelius, S., Schmidt, H.L., (1990). Using isotope fractionation of
533 nitrate-nitrogen and nitrate-oxigen for evaluation of microbial denitrification in sandy aquifer.
534 J. Hydrol. 114, 413-424.

535 Bouwer, H., 2002. Artificial recharge of groundwater: hydrogeology and engineering.
536 Hydrogeol. J. 10, 121-142.

537 Carrey, R., Otero, N., Soler, A., Gomez-Alday, J.J., Ayora, C., (2013). The role of Lower
538 Cretaceous sediments in groundwater nitrate attenuation in central Spain: Column
539 experiments. Appl. Geochem. 32, 142-152.

540 Cey, E.E., Rudolph, D.L., Aravena, R., Parkin, G., (1999). Role of the riparian zone in
541 controllingthe distribution and fate of agricultural nitrogen near a small stream in southern
542 Ontario. J. Contam. Hydrol. 37, 45-67.

543 Clark, I.D., Fritz, P., (1997). Environmental Isotopes in Hydrogeology. Lewis Publishers, New
544 York (352 pp.).

545 Cravotta, C.A., (1997). Use of stable isotopes of carbon, nitrogen and Sulphur to identify
546 sources of nitrogen in surface waters in the lower Susquehanna River Basin, Pennsylvania.
547 U.S. Geological Survey Water-Supply Paper. 2497.

548 Devito, K.J., Fitzgerald, D., Hill, A.R., Aravena, R., (2000). Nitrate dynamics in relation to
549 lithology and hydrologic flow path in a river riparian zone. J. Environ. Qual. 29, 1075-1084.

550 Díaz-Cruz, M.S., Barceló, D., (2008). Trace organic chemicals contamination in ground water
551 recharge. Chemosphere 72 (3): 333-342.

552 Dillon, P.J., (2004). Future management of aquifer recharge. Hydro. Geol. J. 13 (1), 313-316.

553 Dillon, P., Pavelic, P., Toze, S., Rinck-Pfeiffer, S., Martin, R., Knapton, A., Pidsley, D., (2006).
554 Role of aquifer storage in water reuse. Desalination 188 (1-3), 123-134.

555 Dogramaci, S.S., Herczeg, A.L., Schi, S.L., Bone, Y., (2001). Controls on δ34S and δ18O of
556 dissolved sulfate in aquifers of the Murray Basin, Australia and their use as indicators of flow
557 processes. Appl. Geochem. 16, 475-488

558 ENSAT (Enhancement of Soil Aquifer Treatment), (2012). Modelo hidrogeológico: Modelo
559 conceptual de flujo en el sistema de recarga de Sant Vicenç dels Horts, Barcelona: ENSAT.

560 Fox, P., et al. 2006. Advances in Soil Aquifer Treatment Research for Sustainable Water
561 Reuse. Awwa Research Foundation: Denver, 200.

562 Fukada, T., Hiscock, K., Dennis, P.F., Grischek, T., (2003). A dual isotope approach to identify
563 denitrifaction in groundwater at river-bank infiltration site. Water Res. 37, 3070- 3078.

564 Gibert, O., Pomierny, S., Rowe, I., Kalin, R.M., (2008). Selection of organic substrates as
565 potential reactive materials for use in a denitrification permeable reactive barrier (PRB).
566 Bioresources Technol. 99, 7587-7596.

567 Grau-Martínez, A., Torrentó, C., Carrey, R., Rodríguez-Escales, P., Domènech, C., Ghiglieri,
568 G., Soler, A., Otero, N., (2017). Feasibility of two low-cost organic substrates for inducing
569 denitrification in artificial recharge ponds: Batch and flow-through experiments. J. Contam.
570 Hydrol. 198, 48-58

571 Heberer, T., Mechlinski, A., Franck, B., Knappe, A., Massmann, G., Pekdeger, A., Fritz, B.,
572 (2004). Field studies on the fate and transport of pharmaceutical residues in bank filtration.
573 Ground Water Monit. Remediat. 24 (2), 70-77.

574 Horibe, Y., Shigehara, K., Takakuwa, Y., (1973). Isotope separation factors of carbon dioxide
575 water system and isotopic composition of atmospheric oxygen. J. Geophys. Res. 78, 2625-
576 2629.

577 IAEA/WMO (2017). Global Network of Isotopes in Precipitation. The GNIP Database.
578 Accessible at: http://www.iaea.org/water

579 Iribar, V., Carrera, J., Custodio, E., Medina, A., (1997). Inverse modelling of seawater intrusion
580 in the Llobregat delta deep aquifer. J. Hydrol 198 (1-4): 226-244.

581 Kendall, C., Elliott, E.M., Wankel, S.D., (2007).Tracing anthropogenic inputs of nitrogen to
582 ecosystems. (Chapter 12). In: Michener, R.H., Lajtha, K., (Eds), Stable isotopes in Ecology
583 and Environmental Science, second ed. Blackwell Publishing, pp. 375-449.

584 Knöller, K., Vogt, C., Haupt, M., Feisthauer, S., Richnow, H.H., (2011). Experimental
585 investigation of nitrogen and oxygen isotope fractionation in nitrate and nitrite during
586 denitrification. Biogeochemistry 103, 371-384.

587 Knowles, R., (1982). Denitrification. Microbiol. Rev. 46, 43-70.

588 Köck-Schulmeyer, M., Ginebreda, A., Postigo, C., López-Serna, R., Pérez, S., Brix, R., Llorca,
589 M., MLd Alda, Petrovic, M., Munné, A., Tirapu, L., Barceló, D., (2011). Wastewater reuse in
590 Mediterranean semi-arid areas: the impact of discharges of tertiary treated sewage on the
591 load of polar micro pollutants in the Llobregat River (NE Spain). Chemosphere 82(5): 670-
592 678.

593 Krouse, H.R., Mayer, B., (2000). Sulphur and oxygen isotopes in sulphate. In: Cook, P.G.,
594 Hercseg, A.L. (Eds.), Environmnetal Tracers in Subsurface Hydrology. Kluwer Academic
595 Press, Boston, pp.195-231.

596 Lasagna, M., De Luca, D.A., (2016). The use of multilevel sampling techniques for determining
597 shallow aquifer nitrate profiles. Environ. Sci. Pollut. Res. 23 (20) 20431-20448.

598 Lehmann, M.F., Reichert, P., Bernasconi, S.M., Barbieri, A., McKenzie, J.A., (2003). Modelling
599 nitrogen and oxygen isotope fractionation during denitrification in a lacustrine redox-transition
600 zone. Geochim. Cosmochim. Acta 67, 2529-2542.

601 Li, D., Alidina, M., Ouf, M., Sharp, J.O., Saikaly, P., Drewes, J.E., (2013). Microbial community
602 evolution during simulated managed aquifer recharge in response to different biodegradable
603 dissolved organic carbon (BDOC) concentrations. Water Res. 47 (7), 2421-2430.

604 Liu, Y.-S., G.-G. Ying, A. Shareef, and R. S. Kookana, (2013), Biodegradation of three
605 selected benzotriazoles in aquifer materials under aerobic and anaerobic conditions, J.
606 Contam. Hydrol., 151, 131–139.

607 Maeng, S.K., Sharma, S.K., Lekkerkerker-Teunissen, K., Amy, G.L., (2011). Occurrence and
608 fate of bulk organic matter and pharmaceutically active compounds in managed aquifer
609 recharge: a review. Water Res. 45 (10), 3015-3033.

610 Mariotti, A., Germon, J.C., Hubert, P., Kaiser, P., Letolle, R., Tardieux, P., (1981).
611 Experimental determination of nitrogen kinetic isotope fractionation: some principles,
612 illustration for the denitrification and nitrification processes. Plant Soil 62, 413-430.

613 Mariotti, A., Landreau, A., Simon, B., (1988). 15N isotope biogeochemistry and natural
614 denitrification process in groundwater application to the chalk aquifer of northern France.
615 Geochim. Cosmochim. Acta 52, 1869-1878

616 Massmann, G., Greskowiak, J., Dunnbier, U., Zuehlke, S., Knappe, A., Pekdeger, A., (2006).
617 The impact of variable temperatures on the redox conditions and the behaviour of
618 pharmaceutical residues during artificial recharge. J. Hydrol., 328 (1-2): 141- 156.

619 McIlvin, M.R., Altabet, M.A., (2005). Chemical conversion of nitrate and nitrite to nitrous oxide
620 for nitrogen and oxygen isotopic analysis in freshwater and seawater. Anal. Chem. 77, 5589-
621 5595.

622 Menció, A., Mas-Pla, J., Soler, A., Regàs, O., Boy-Roure, M., Puig, R., Bach, J., Domènech,
623 C., Folch, A., Zamarona, M., Brusi, D., (2016). Nitrate pollution of groundwater; all right…, but
624 nothing else? Sci. Total Environ. 539C: 241-251.

625 Mengis, M., Schif, S.L., Harris, M., English, M.C., Aravena, R., Elgood, R.J, MacLean, A.,
626 (1999). Multiple geochemical and isotopic approaches for assessing ground water NO3
627 elimination in a riparian zone. Ground Water 37, 448-457.

628 Miller, J.H., Ela, W.P., Lansey, K.E., Chipello, P.L., Arnold, R.G., (2006). Nitrogen
629 transformations during soil-aquifer treatment of wastewater effluent-oxygen effects in field
630 studies. J. Environ. Eng. Asce 132 (10): 1298-1306.

631 Otero, N., Soler, A., Canals, A., (2008). Controls of δ34S and δ18O in dissolved sulphate:
632 learning from a detailed survey in the Llobregat River (Spain). Appl. Geochm. 23, 1166-1185.

633 Otero, N., Torrentó, C., Soler, A, Menció, A., Mas-Pla, J., (2009). Monitoring groundwater
634 nitrate attenuation in a regional system coupling hydrogeology with multi-isotopic methods:
635 the case of Plana de Vic (Osona, Spain). Agric. Ecosyst. Environ. 133 (1-2), 103-113.

636 Parkhurst, DL, Appelo, CAJ (2012) Description of input and examples for PHREEQC version
637 3a computer program for speciation, batch-reaction, one-dimensional transport, and inverse
638 geochemical calculations. USGS Techniques and Methods, book 6, chap. A43, 497 p.,
639 available only at http://pubs.usgs.gov/tm/06 A43/.

640 Pauwels, H., Foucher, J.C., and Kloppmann, W. (2000). Denitrification and mixing in a schist
641 aquifer: influence on water chemistry and isotopes. Chem. Geol. 168, 307-324.

642 Pauwels, H., Ayraud-Vergnaud, V., Aquilina, L., and Molénat, J. (2010). The fate of nitrogen
643 and sulfur in hard-rock aquifers as shown by sulfate-isotope tracing. Appl. Geochem. 25, 105-
644 115.

645 Pauwels, H., Kloppmann, W., Foucher, J.C., Martelat, A., and Fritsche, V. (1998). Field tracer
646 test for denitrification in a pyrite-bearing schist aquifer. Appl. Geochem. 13, 284-292.

647 Patterson, B., Shackleton, M., Furness, A., Bekele, E., Pearce, J., Linge, K., Busetti, F.,
648 Spadek, T., Toze, S., (2011). Behaviour and fate on nine recycled water trace organics during
649 managed aquifer recharge in aerobic aquifer. J. Contam. Hydrol. 122 (1-4), 53-62.

650 Pierre, C., Taberner, C., Urquiola, M.M., Pueyo, J.J., (1994). Sulphur and oxygen isotope
651 composition of sulphates in hypersaline environments, as markers of redox depositional
652 versus diagenetic changes. Mineral Mag. 58, 724-725.

653 Quevauviller, P.P., Fouillac, A.M., Grath, J., Ward, R., (2009). Groundwater monitoring, Wiley,
654 New York. ISBN: 978-0-470-74969-2.

655 Rodríguez-Escales, P., Folch, A., van Breukelen, B.M., Vidal-Gavilan, G., Sanchez-Vila, X.,
656 (2016a). Modeling long term enhanced in situ biodenitrification and induced heterogeneity in
657 column experiments under different feeding strategies. J. Hydrol. 538, 127-137.

658 Rodríguez-Escales, P., Folch, A., Vidal-Gavilan, G., van Breukelen, B.M. (2016b). Modeling
659 biogeochemical processes and isotope fractionation of enhanced in situ biodenitrification in a
660 fractured aquifer. Chem. Geol., 425, 52-64.

661 Rodríguez-Escales, P., Fernàndez-Garcia, D., Drechsel, J., Folch, A., Sanchez-Vila, X.
662 (2017). Improving degradation of emerging organic compounds by applying chaotic advection
663 in Managed Aquifer Recharge in randomly heterogeneous porous media. Water Resour. Res.,
664 53 (5), 4376-4392.

665 Ryabenko, E., Altabet, M.A., Wallace, D.W.R., (2009). Effect of chloride on the chemical
666 conversion of nitrate to nitrous oxide for δ15N analysis. Limnol. Oceanogr. 7, 545-552.

667 Schmidt, C.M., Fisher, A.T., Racz, A., Wheat, C.G., Los Huertos, M., Lockwood, B., (2012).
668 Rapid nutrient load reduction during infiltration of managed aquifer recharge in an agricultural
669 groundwater basin: Pajaro Valley, California. Hydrol. Process. 26, 2235-2247.

670 Schmidt, C.S., Richardson, DJ., Baggs, E.M., (2011). Constraining the conditions conducive
671 to dissimilatory nitrate reduction to ammonium in temperate arable soils. Soil Biol. Biochem.
672 43, 1607-1611.

673 Sine S.E., (2017) Paradigm shift: does river metabolism mask the isotopic signal of nitrate
674 sources? MSc. Thesis. University of Waterloo. 118 p.

675 Solà, V., (2009). Actualització hidroquímica I isotòpica dels aqüífers del Baix Llobregat per a
676 la determinació de la intrusió marina, amb consideració de la isotopia del sulfat. Tesi de
677 Màster en Hidrologia Subterrània.

678 Sprenger, C., Hartog, N., Hernández, M., Vilanova, E., Grützmacher, G., Scheibler, F.,
679 Hannappel, S., (2017) Inventory of managed aquifer recharge sites in Europe: historical
680 development, current situation and perspectives. Hydrogeol J, 25, 1909-1922

681 Torrentó, C., Urmeneta, J., Otero, N., Soler, A., Viñas, M., Cama, J., (2011). Enhanced
682 denitrification in groundwater and sediments from a nitrate-contaminated aquifer after addition
683 of pyrite. Chem. Geol. 287, 90-101.

684 Utrilla, R., Pierre, C., Orti, F., Pueyo, J.J., (1992). Oxygen and sulphur isotope compositions
685 as indicators of the origin of Mesozoic and Cenozoic evaporites from Spain. Chem. Geol. Isot.
686 Geosci. 102, 229-244.

687 Valhondo, C., Carrera, J., Ayora, C., Barbieri, M., Noedler, K., Licha, T., Huerta, M., (2014).
688 Behavior of nine selected emerging trace organic contaminants in an artificial recharge system
689 supplemented with a reactive barrier. Environ. Sci. Pollut. R. 21, 11832-11843

690 Valhondo, C., Carrera, J., Ayora, Tubau, I., Martinez-Landa, L., Nödler, K., Licha, T., (2015).
691 Characterizing redox conditions and monitoring attenuation of selected pharmaceuticals
692 during artificial recharge through a reactive layer. Sci. Total Environ. 512-513, 240-250.

693 Valhondo, C., Martinez-Landa, L., Carrera, J., Hidalgo, J.J., Tubau, I., De Pourcq, K., Grau-
694 Martínez, A., Ayora, C., (2016). Tracer test modeling for local scale residence time distribution
695 characterization in an artificial recharge site. Hydrol.Earth Syst.Sci. 20, 4209-4221.

696 Valhondo, C., Martinez-Landa, L., Carrera J., Ayora, c., Nödler, K., Licha. T., (2018).
697 Evaluation of EOC removal processes during artificial recharge through a reactive barrier. Sci.
698 Total Environ. 612, 985-994.

699 Vanderzalm, J., Salle, C.L.G.L., Dillon, P., (2006). Fate of organic matter during aquifer
700 storage and recovery (ASR) of reclaimed water in a carbonate aquifer. Appl. Geochem. 21
701 (7), 1204-1215.

702 Vàzquez-Suñé, E., Capino, B., Abarca, E., Carrera, J., (2007). Estimation of recharge from
703 floods in disconnected stream-aquifer systems, Ground Water, 45 (5), 579-589.

704 Vitòria, L., Otero, N., Canals, A., Soler, A., (2004). Fertilizer characterization: isotopic data (N,
705 S, O, C and Sr). Environ. Sci. Technol. 38, 3254-3262.

706 Vogel, J.C., Ehhalt, D.H., (1963). The use of carbon isotopes in groundwater studies. In
707 Radioisotopes in Hydrology. Vienna: International Atomic Energy Agency, pp. 338-396.

708 Xue, D., Botte, J., De Baets, B., Accoe, F., Nestler, A., Taylor, P., Van Cleemput, O., Berglund,
709 M., Boeckkx, P., (2009). Present limitations and future prospects of stable isotopes methods
710 for nitrate source identification in surface and groundwater. Water Res. 43, 1159-1170.

Figure 1

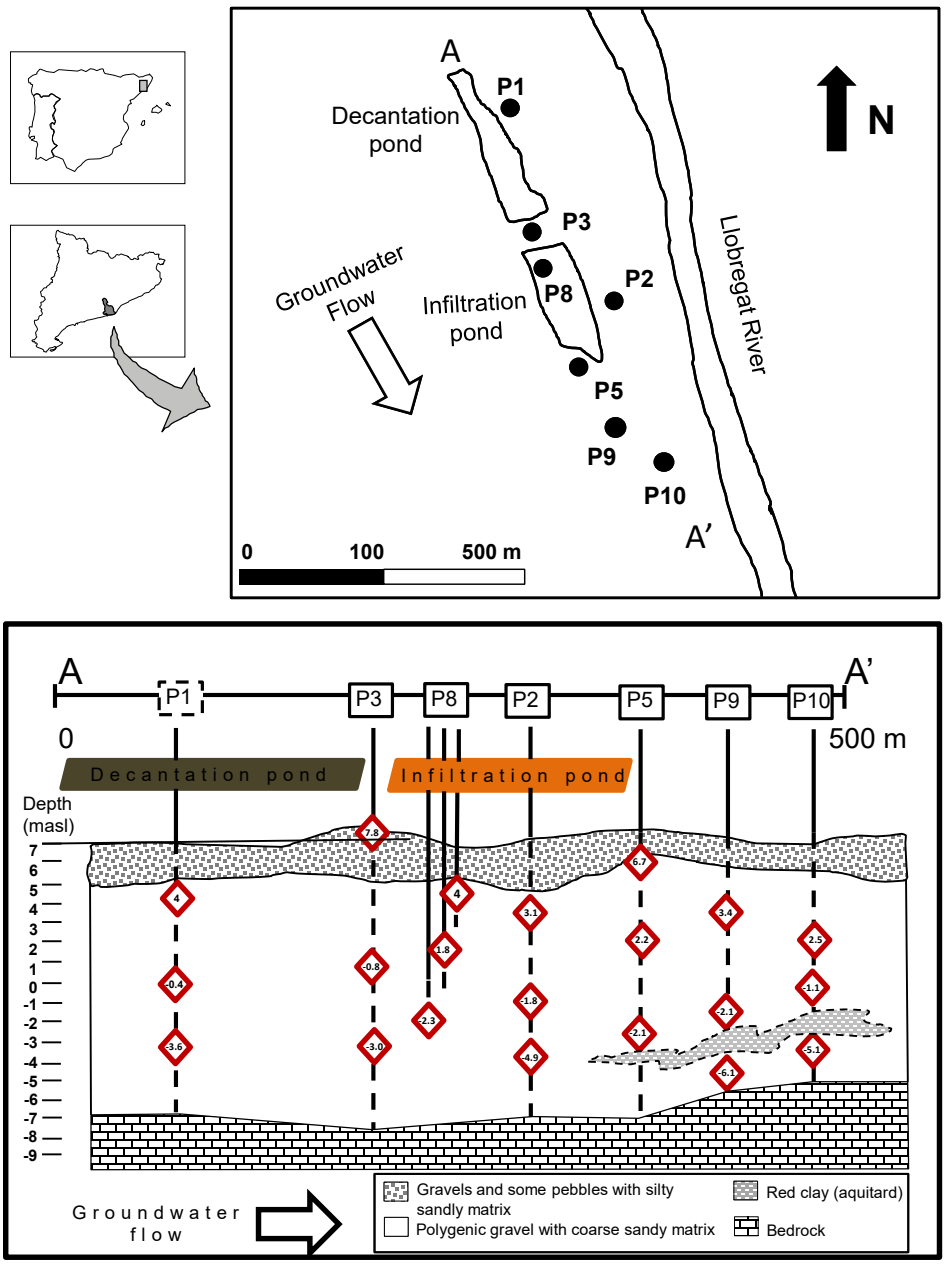
A
P1
Decantation pond
P3
P8
P2
Infiltration pond
Groundwater Flow
P5
P9
P10
A'
Llobregat River
N
0
100
500 m
A
P1
P3
P8
P2
P5
P9
P10
A'
0
500 m
Decantation pond
Infiltration pond
Depth (masl)
Groundwater flow
Gravels and some pebbles with silty sandly matrix
Polygenic gravel with coarse sandy matrix
Red clay (aquitard)
Bedrock

Figure 2

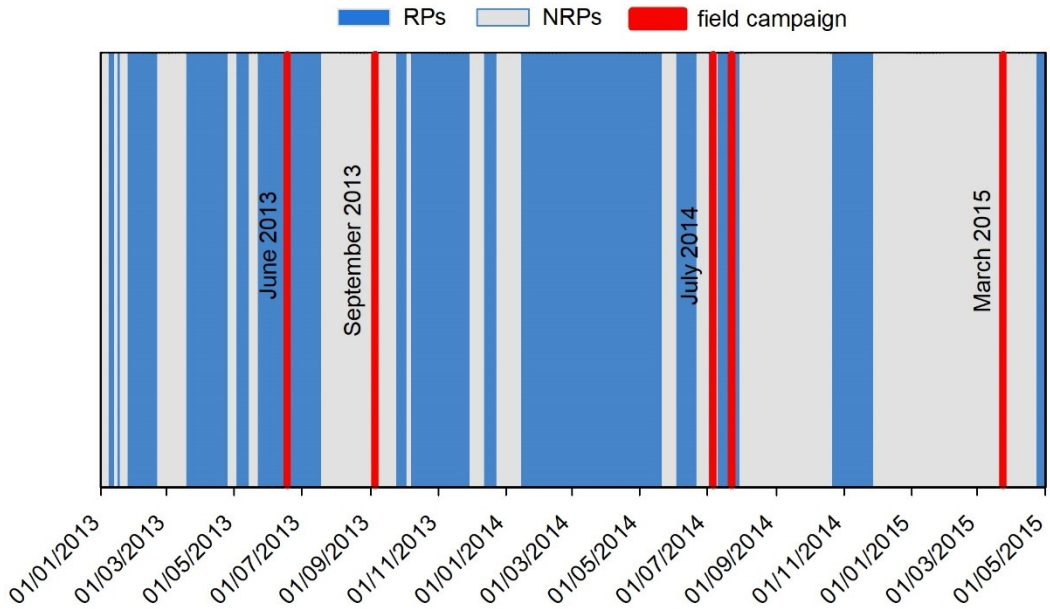
RPs
NRPs
field campaign
June 2013
September 2013
July 2014
March 2015
01/01/2013
01/03/2013
01/05/2013
01/07/2013
01/09/2013
01/11/2013
01/01/2014
01/03/2014
01/05/2014
01/07/2014
01/09/2014
01/11/2014
01/01/2015
01/03/2015
01/05/2015

Figure 3

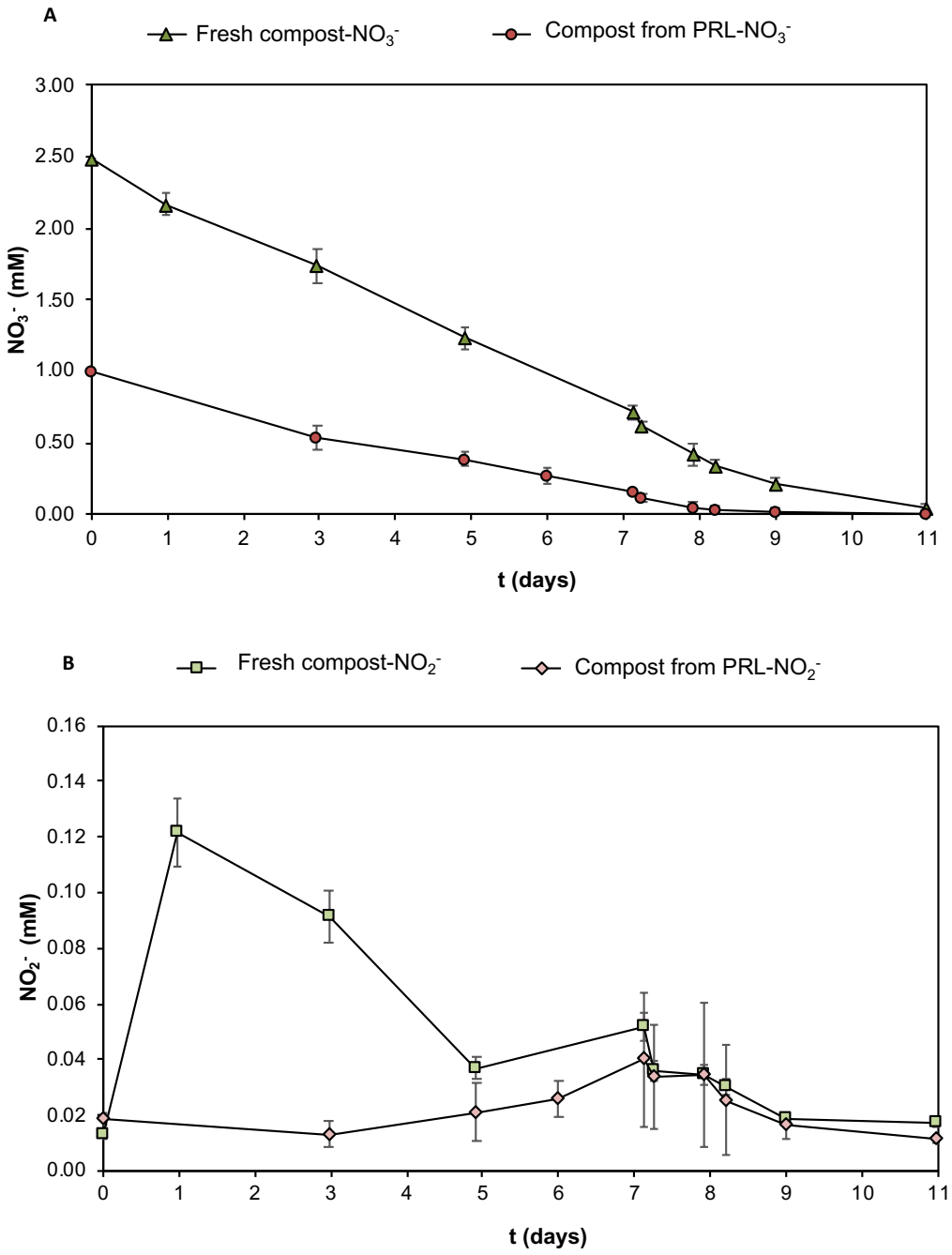
A
Fresh compost-NO3-
Compost from PRL-NO3-
NO3- (mM)
t (days)
B
Fresh compost-NO2-
Compost from PRL-NO2-
NO2- (mM)
t (days)

Figure 4

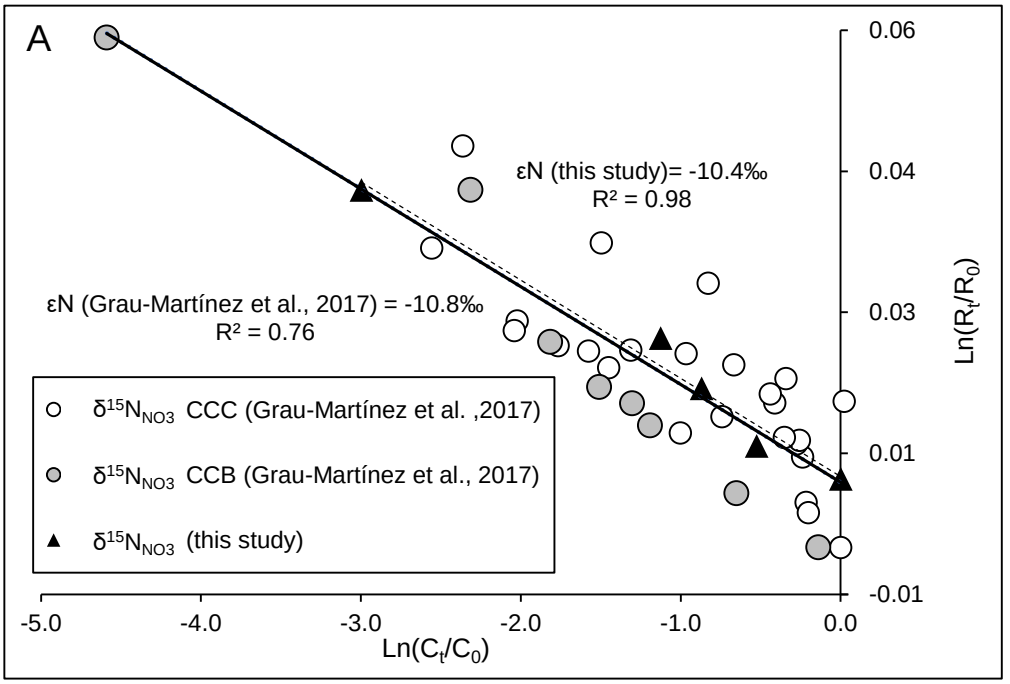
A
εN (this study)= -10.4‰
R² = 0.98
εN (Grau-Martínez et al., 2017) = -10.8‰
R² = 0.76
δ15NNO3 CCC (Grau-Martínez et al. ,2017)
δ15NNO3 CCB (Grau-Martínez et al., 2017)
δ15NNO3 (this study)
0.06
0.04
0.03
0.01
-0.01
-5.0
-4.0
-3.0
-2.0
-1.0
0.0
Ln(Ct/C0)
Ln(Rt/R0)

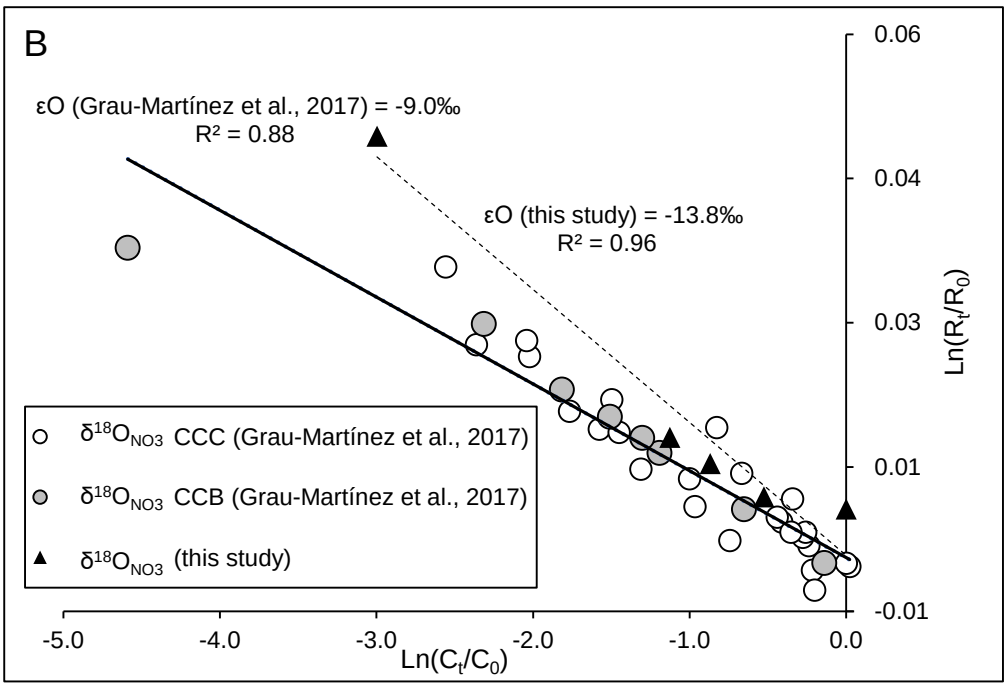
B
εO (Grau-Martínez et al., 2017) = -9.0‰
R² = 0.88
εO (this study) = -13.8‰
R² = 0.96
δ18ONO3 CCC (Grau-Martínez et al., 2017)
δ18ONO3 CCB (Grau-Martínez et al., 2017)
δ18ONO3 (this study)
0.06
0.04
0.03
0.01
-0.01
-5.0
-4.0
-3.0
-2.0
-1.0
0.0
Ln(Ct/C0)
Ln(Rt/R0)

Figure 5

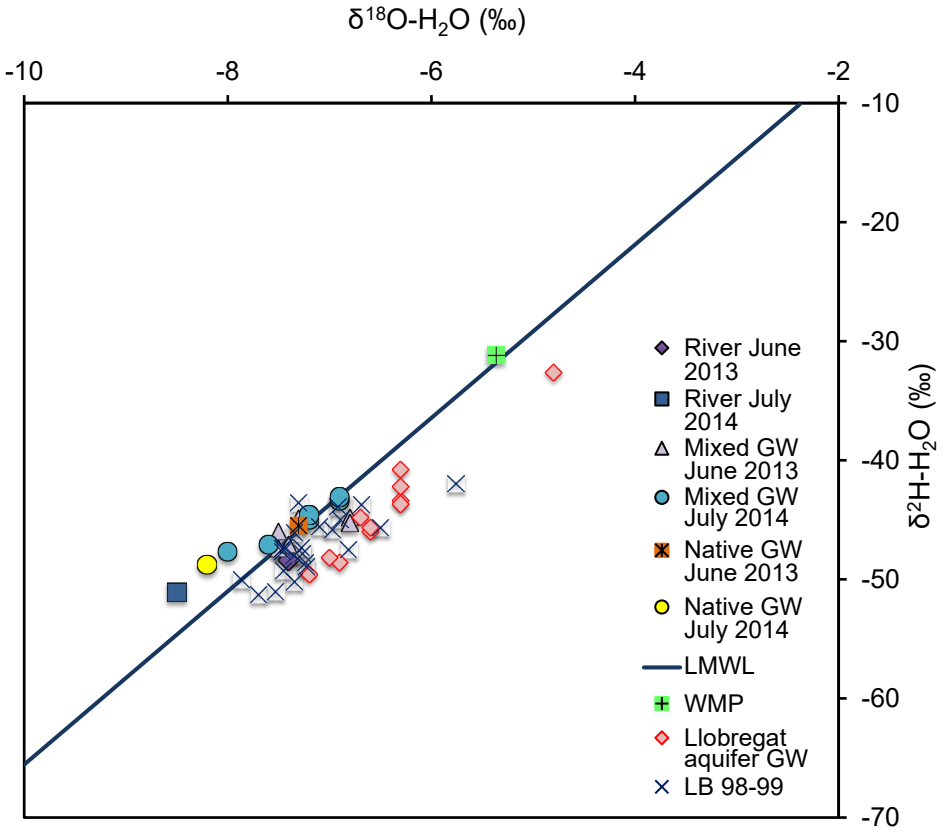
δ18O-H2O (‰)
-10
-8
-6
-4
-2
-10
-20
-30
-40
-50
-60
-70
δ2H-H2O (‰)
River June 2013
River July 2014
Mixed GW June 2013
Mixed GW July 2014
Native GW June 2013
Native GW July 2014
LMWL
WMP
Llobregat aquifer GW
LB 98-99

Figure 6

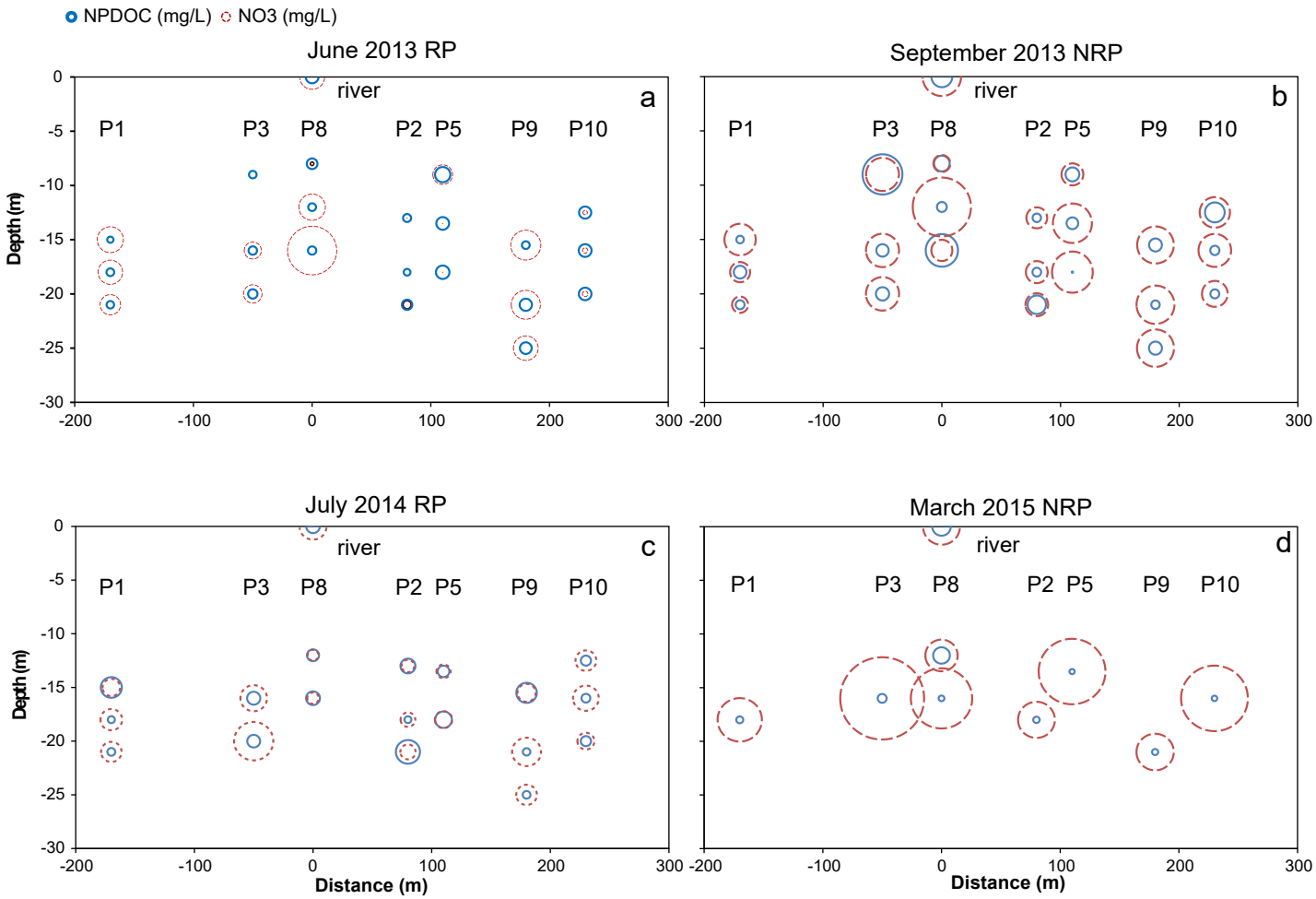
NPDOC (mg/L)
NO3 (mg/L)
June 2013 RP
September 2013 NRP
July 2014 RP
March 2015 NRP
river
a
b
c
d
P1
P3
P8
P2
P5
P9
P10
Depth (m)
Distance (m)
0
-5
-10
-15
-20
-25
-30
-200
-100
0
100
200
300

Figure 7

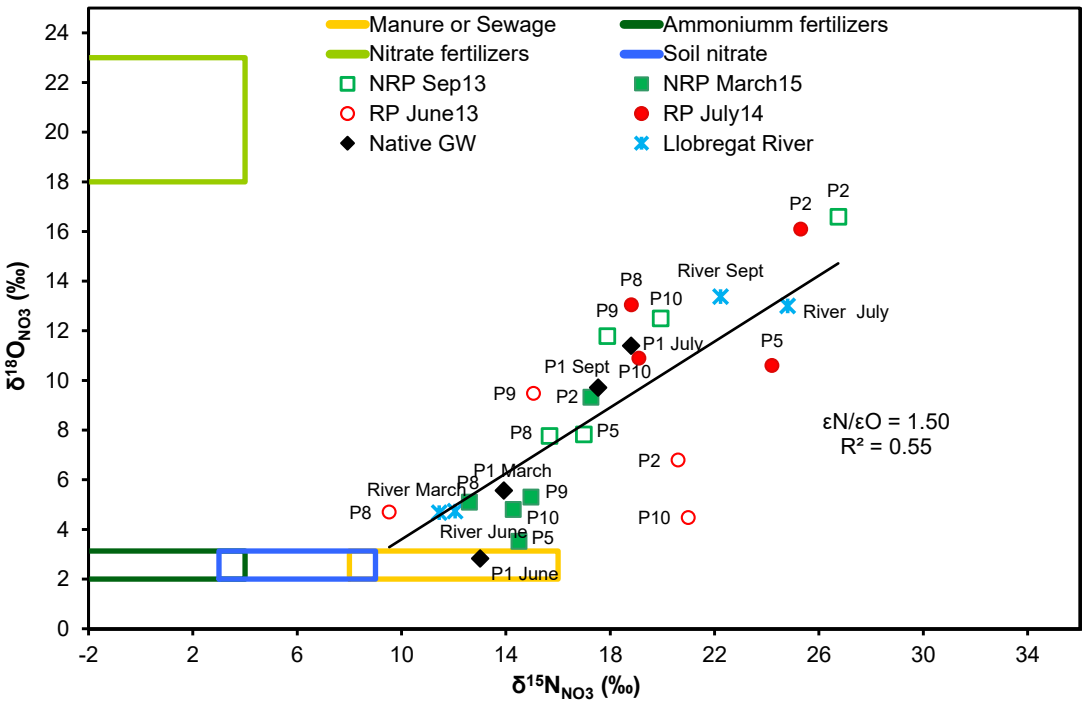
Manure or Sewage
Ammoniumm fertilizers
Nitrate fertilizers
Soil nitrate
NRP Sep13
NRP March15
RP June13
RP July14
Native GW
Llobregat River
δ18ONO3 (‰)
δ15NNO3 (‰)
εN/εO = 1.50
R² = 0.55
P2
P8
P10
P9
River Sept
River July
P1 July
P5
P1 Sept
P1 March
River March
River June
P1 June

Figure 8

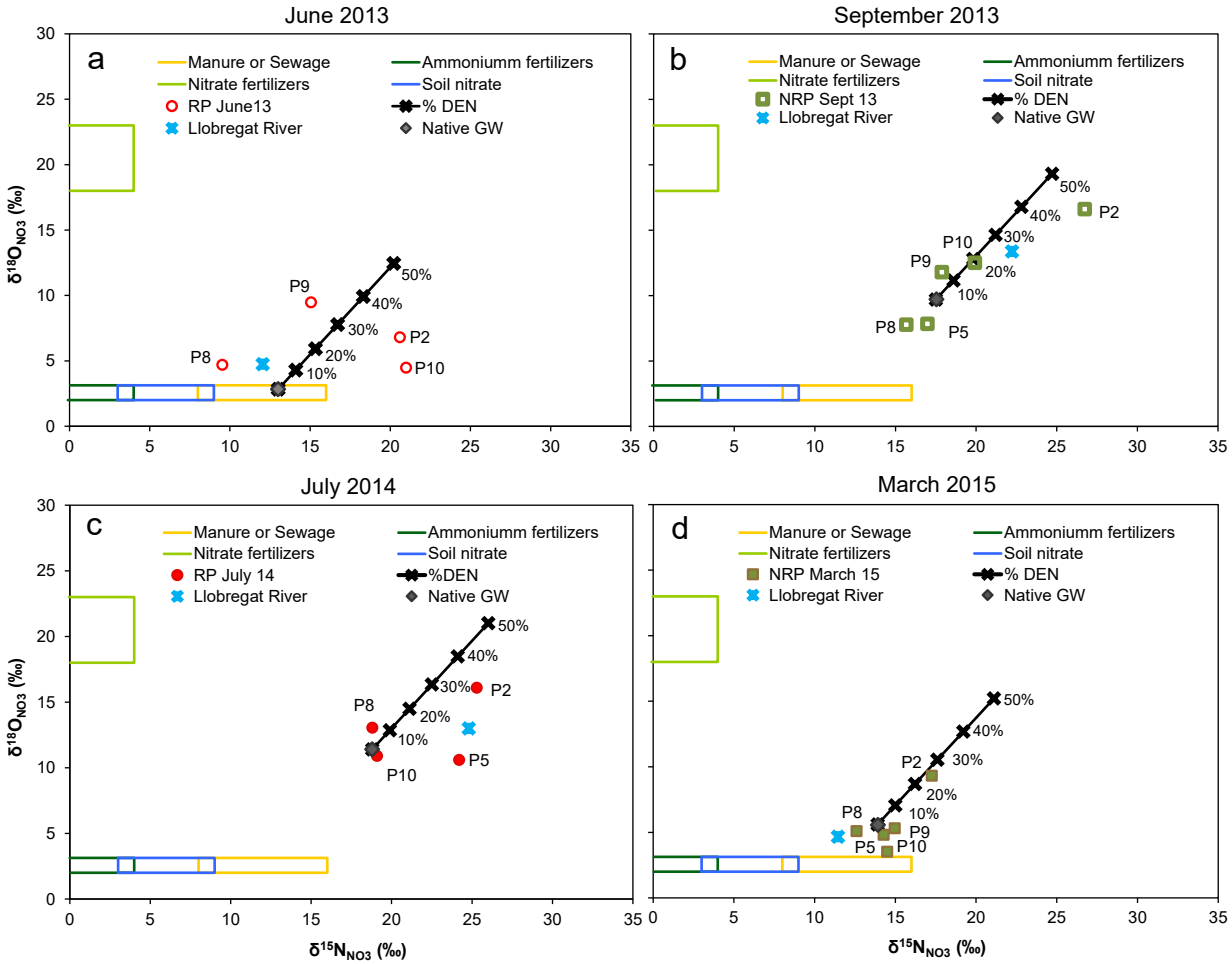
June 2013
a
Manure or Sewage
Nitrate fertilizers
RP June13
Llobregat River
Ammoniumm fertilizers
Soil nitrate
% DEN
Native GW
P9
P8
P2
P10
50%
40%
30%
20%
10%
September 2013
b
Manure or Sewage
Nitrate fertilizers
NRP Sept 13
Llobregat River
Ammoniumm fertilizers
Soil nitrate
% DEN
Native GW
P2
P10
P9
P8
P5
July 2014
c
Manure or Sewage
Nitrate fertilizers
RP July 14
Llobregat River
Ammoniumm fertilizers
Soil nitrate
%DEN
Native GW
P8
P2
P5
P10
March 2015
d
Manure or Sewage
Nitrate fertilizers
NRP March 15
Llobregat River
Ammoniumm fertilizers
Soil nitrate
% DEN
Native GW
P2
P8
P9
P5
P10
δ18ONO3 (‰)
δ15NNO3 (‰)

Figure 9

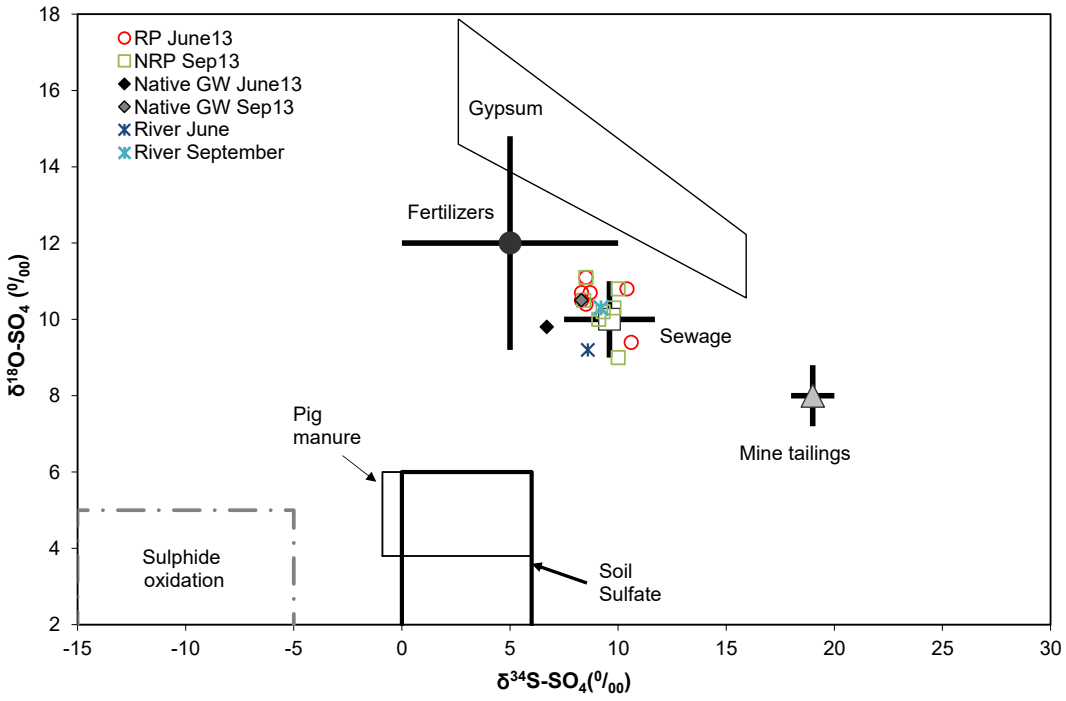
RP June13
NRP Sep13
Native GW June13
Native GW Sep13
River June
River September
Gypsum
Fertilizers
Sewage
Mine tailings
Pig manure
Sulphide oxidation
Soil Sulfate
δ18O-SO4 (0/00)
δ34S-SO4(0/00)
18
16
14
12
10
8
6
4
2
-15
-10
-5
0
5
10
15
20
25
30

Figure 10

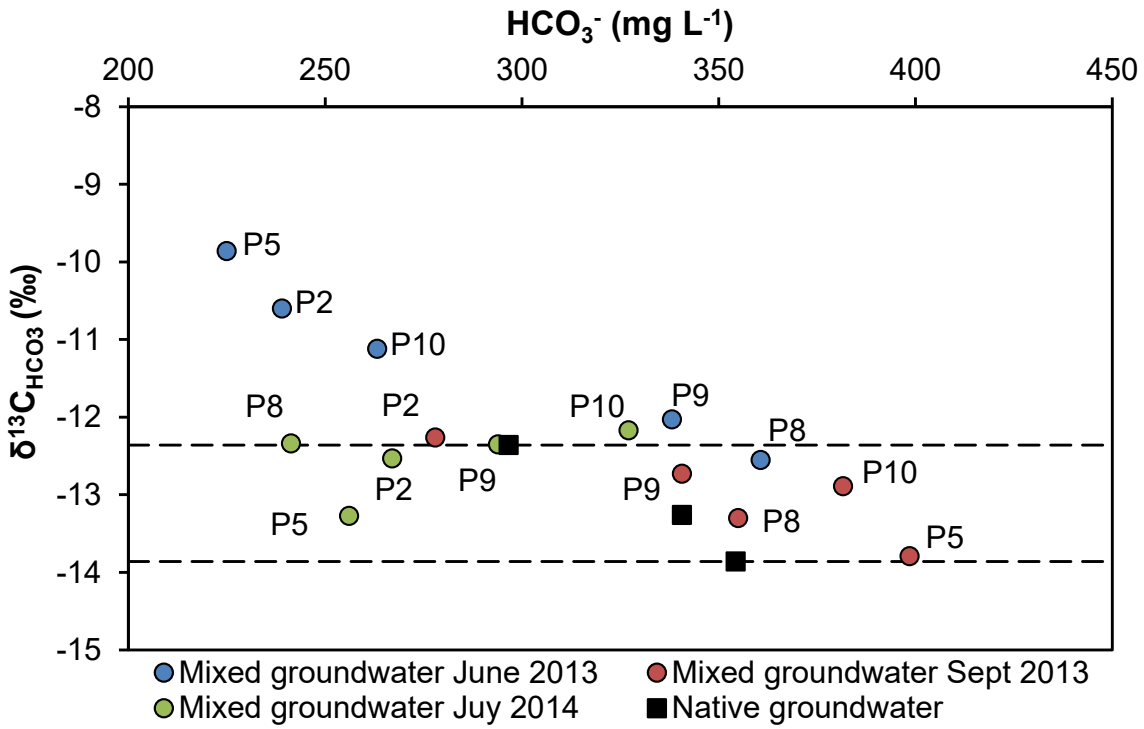
HCO3- (mg L-1)
200
250
300
350
400
450
-8
-9
-10
-11
-12
-13
-14
-15
δ13CHCO3 (‰)
P5
P2
P10
P8
P2
P10
P9
P8
P2
P9
P9
P10
P5
P8
P5
Mixed groundwater June 2013
Mixed groundwater Sept 2013
Mixed groundwater Juy 2014
Native groundwater

Supplementary material

Monitoring induced denitrification during managed aquifer recharge in an infiltration pond

Alba Grau-Martínez[a], Albert Folch[b,c], Clara Torrentó[a,d], Cristina Valhondo[c,e], Carme Barba[b,c], Cristina Domènech[a], Albert Soler[a], Neus Otero[a,f]

[a]*Grup de Mineralogia Aplicada i Geoquímica de Fluids, Departament de Mineralogia, Petrologia i Geologia Aplicada, SIMGEO UB-CSIC, Facultat de Ciències de la Terra, Universitat de Barcelona (UB), C/ Martí i Franquès, s/n - 08028 Barcelona, Spain.*

[b]*Department of Civil and Environmental Engineering (DECA), Universitat Politècnica de Catalunya (UPC), c/Jordi Girona 1-3, 08034 Barcelona, Spain.*

[c]*Associated Unit: Hydrogeology Group (UPC-CSIC).*

[d]*Centre for Hydrogeology and Geothermics, University of Neuchâtel, Rue Emile-Argand 11, 2000 Neuchâtel, Switzerland.*

[e]*Institute of Environmental Assessment and Water Research (IDAEA), CSIC, c/ Jordi Girona 18, 08034 Barcelona, Spain.*

[f]*Serra Hunter Fellow, Generalitat de Catalunya, Spain.*

(*) Corresponding author: Alba Grau-Martínez

e-mail: albagrau@ub.edu

Phone: +34 93 403 37 73 Fax: +34 93 402 13 40.

Total number of pages (including cover): 8

Tables: 5

Figures: 2

Table S1: Characterization of the reactive layer material

Summary of key parameters of the organic substrate used in the reactive layer of the MAR pond

Organic substrate	N (%)	C_{total} (%)	$\delta^{15}N$ (‰)	$\delta^{13}C$ (‰)
PRL	1.0±0.2	15.1±1.1	12.1±1.1	-25.1±0.2

Table S2: Results of batch experiments

Chemical and isotopic characterization of the outflow water of the batch experiments: CC experiments with fresh commercial compost (Grau-Martínez et al., 2017) and PRL experiments with two-year-old material extracted from the PRL. Concentration values are shown as the average of the triplicate experiments.

Code	t (d)	NO_3^- (mM)	NO_2^- (mM)	$\delta^{15}N_{NO3}$ (‰)	$\delta^{18}O_{NO2}$ (‰)
CC-1	0	2.5±0.00	0.01±0.01	n.d.	n.d.
CC-2	1	2.2±0.08	0.12±0.01	+9.4	+18.6
CC-3	3	1.7±0.12	0.09±0.01	+15.2	+24.3
CC-4	4.9	1.2±0.08	0.04±0.01	+22.6	+30.3
CC-5	7.1	0.7±0.05	0.05±0.00	+25.0	+32.0
CC-6	7.3	0.6±0.03	0.04±0.01	+26.8	+34.3
CC-7	7.9	0.4±0.08	0.03±0.00	+31.7	+37.2
CC-8	8.2	0.3±0.04	0.03±0.00	+48.5	+44.3
CC-9	9	0.2±0.04	0.02±0.00	+65.6	+52.6
CC-10	11	0.1±0.02	0.02±0.01	n.d.	n.d.
PRL-1	0	1.0±0.00	0.02±0.00	+16.8	+24.4
PRL-2	3	0.5±0.09	0.01±0.00	+20.4	+25.7
PRL-3	4.9	0.4±0.05	0.02±0.01	+26.6	+29.3
PRL-4	6	0.3±0.06	0.03±0.01	+32.1	+32.1
PRL-5	7.1	0.2±0.01	0.04±0.02	+48.5	+64.9
PRL-6	7.3	0.1±0.03	0.03±0.02	n.d.	n.d.
PRL-7	7.9	0.1±0.04	0.03±0.03	n.d.	n.d.
PRL-8	8.2	0.0±0.03	0.03±0.02	n.d.	n.d.
PRL-9	9	0.0±0.04	0.02±0.00	n.d.	n.d.
PRL-10	11	0.0±0.01	0.01±0.00	n.d.	n.d.

(n.d.: not determined)

Table S3: Chemicals results of field campaigns

Chemical characterization of the groundwater and river water samples collected during the four field campaigns (including principal physico-chemicals parameters, major cations, major anions and NPDOC).

Piez	Depth (m)	pH	Cond (µS/cm)	NPDOC (mg/L)	NO_3^- (mg/L)	SO_4^{2-} (mg/L)	Cl^- (mg/L)	HCO_3^- (mg/L)	Ca^{2+} (mg/L)	Na^{2+} (mg/L)	Fe (mg/L)
June 2013											
P1 (NGW)	13	7.43	989	2	6.4	133.3	116.2	335.4	125.7	93.6	0.07
P1 (NGW)	18	7.23	997	2.3	6	112.1	104.2	340.6	126.5	95.4	0.04
P1 (NGW)	21	7.26	987	2.3	5	117.3	105.6	334.1	122.3	95.6	0.08
P2	13	7.59	1026	2.4	0	130.9	131	243.6	111.9	102.9	0.04
P2	18	7.6	1028	2.1	0	127.9	135.7	239	111	103.2	0.04
P2	21	7.62	1001	3	1.9	130.3	131.5	227.1	104.3	101.4	0.06
P3	9	7.43	1148	2.3	0	125.6	139.6	345.1	137.6	114.8	n.d.
P3	16	7.27	1149	2.5	4.2	121.5	132.8	348.2	134.9	114.6	n.d.
P3	20	7.2	1151	2.7	4.6	105.7	130.8	347.3	124.4	107	n.d.
P5	9	7.56	1031	4.1	4.9	132.3	135.7	227.3	99.5	109.9	0.51
P5	13.5	7.53	1007	3.5	0	126.7	133.8	225	89.4	102.4	0.05
P5	18	7.45	1003	3.7	0	122.9	134	218.1	98.4	77.4	0.05
P8	8	7.55	1010	3	0.9	103.3	122.4	243.8	123.9	79.9	0.03
P8	12	7.28	1170	2.3	6.5	119.4	127.8	360.6	160.6	92.6	0.02
P8	16	7.4	n.d.	2.5	11.9	231.4	227.4	412.4	126.6	115	0.09
P9	15.5	7.26	1289	2.3	7.3	132.6	153.6	334.1	121.2	108	0.05
P9	21	7.24	1297	3.4	7.1	131.8	157.8	338.1	129	107.4	0.01
P9	25	7.34	1265	3.3	6.1	133.1	149.6	328.8	101.8	106.3	0.03
P10	12.5	7.54	1024	3.4	1.2	107	121.2	269	100.6	72.4	0.02
P10	16	7.39	1017	3.5	19.4	108.9	118.4	263.2	105.1	74.8	0.03
P10	20	7.42	1017	3.5	1.5	124.6	124.6	258.4	99.7	74.1	0.02
River	-	8.24	1094	3.5	6.1	119.1	99.7	239.33	102.5	77.2	n.d.
September 2013											
P1 (NGW)	13	7.26	1228	2.0	6.9	135.9	153.4	327.5	113.9	85.7	0.02
P1 (NGW)	18	7.21	1216	3.0	4.5	109.7	143.5	296.6	105.5	88.5	0.02
P1 (NGW)	21	7.24	1213	2.3	3.7	125.2	163.2	294.9	102.4	89.2	0.02
P2	13	7.26	1230	2.2	4.7	128.4	173.9	282.1	104.5	88.8	0.02
P2	18	7.28	1231	2.2	4.9	129	175.9	278	104.8	90.4	0.01
P2	21	7.34	1233	4.2	5.1	129.8	171.5	286	104.3	89.1	0.01
P3	9	7.41	1253	8.6	7.2	117.5	176.5	363	117.2	100.2	n.d.
P3	16	7.23	1245	3.0	7.2	113.7	176.4	364.6	117.3	99.7	n.d.
P3	20	7.14	1266	3.1	7.3	122	175.5	368.7	117.5	98.6	n.d.

P5	9	7.22	1351	3.3	4.9	137.9	177.3	357.4	105.4	99.7	0.01
P5	13.5	7.15	1466	2.8	8.5	164.4	179.2	398.5	121.9	107.8	0.01
P5	18	7.15	1433	0.1	8.8	160	177.4	391.2	123.4	107.6	0.03
P8	8	7.19	1150	3.6	3.9	143	175.2	277.7	99.8	94.2	0.01
P8	12	7.12	1270	2.5	12.4	191.3	184.7	354.9	118.8	99.6	0.01
P8	16	7.14	1451	7.1	4.8	139.5	175.2	406.1	138.2	114.3	0.03
P9	15.5	7.24	1286	3.1	8.0	173.3	177.9	354.4	116.1	110.2	0.03
P9	21	7.2	1311	2.2	8.3	168.2	177.8	340.6	113.8	107.5	0.02
P9	25	7.16	1313	3.1	8.1	167.3	182.1	355	117.6	109.1	0.01
P10	12.5	7.3	1359	4.5	6.7	162.6	190.3	381.3	116	114.7	0.02
P10	16	7.1	1376	2.3	7.2	167.5	191.6	381.6	114.4	112.2	0.00
P10	20	7.1	1364	2.3	5.7	164.8	191.1	382.3	118.2	118.2	0.01
River	-	7.9	1120	4.7	8.4	128.6	235.7	227.2	88.8	124	n.d.
July 2014											
P1 (NGW)	13	7.11	1584	4.9	4.2	181.1	241.6	228.5	135.2	136.1	0.02
P1 (NGW)	18	7.05	1557	1.9	5.0	173	224.7	354.3	135.2	138.9	0.03
P1 (NGW)	21	7.13	1566	2.1	4.8	180.7	223.4	357	132	132.3	0.03
P2	13	7.3	1507	3.6	3.1	140.7	267	261.2	94.2	153.8	0.03
P2	18	7.36	1512	1.9	3.5	150.9	261	267	98.9	153.8	0.03
P2	21	7.28	1518	5.5	3.6	138.3	212	272.6	103.4	158.1	0.01
P3	9	n.d.	n.d.	n.d.	n.d.	n.d.	n.d.	n.d.	n.d.	n.d.	n.d.
P3	16	7.15	1653	3.2	6.1	168.6	241	399	144.1	142.4	n.d.
P3	20	7.15	1678	3.2	8.7	168.6	241.6	385.8	141.2	143.9	n.d.
P5	9	n.d.	n.d.	n.d.	n.d.	n.d.	n.d.	n.d.	n.d.	n.d.	n.d.
P5	13.5	7.39	1556	2.9	3.4	133.8	274.6	256.1	97.4	163.3	0.02
P5	18	7.42	1543	4.0	4.1	147.8	269.6	255.2	96.7	165	0.02
P8	8	n.d.	n.d.	n.d.	n.d.	n.d.	n.d.	n.d.	n.d.	n.d.	n.d.
P8	12	7.45	1479	3.0	2.8	120	267.5	241.3	92.4	159.9	0.02
P8	16	7.39	1542	3.4	2.9	152	262.7	253.8	99.8	161.1	0.02
P9	15.5	7.3	1565	4.8	4.3	152.8	256.5	301	102.8	158.5	0.02
P9	21	7.32	1551	2.0	6.6	131.5	249.5	293.9	105.2	157.9	0.02
P9	25	7.22	1587	2.1	4.8	175.9	249.3	316.7	112.8	151.3	0.02
P10	12.5	7.23	1666	2.6	4.8	172.1	266.8	340.4	133.1	168.1	0.06
P10	16	7.28	1652	2.3	5.9	179.9	265.4	327.1	123.2	162.7	0.01
P10	20	7.25	1641	2.6	4.0	147.2	224.2	317.7	123.2	166.7	0.05
River	-	8.46	1362	3.3	6.1	146	223.2	194	98.9	135.6	n.d.
March 2015											
P1 (NGW)	18	7.36	1332	1.9	9.8	181.4	212.3	382.6	142.6	116.2	0.01
P2	18	7.34	1273	1.8	8.2	139.6	211.8	314.2	121.4	113.5	0.00
P5	18	6.98	1369	1.5	14.6	200.3	191.6	408.1	141.8	163.3	0.02
P8	12	7.13	1235	4.0	7.3	141.2	186.1	379.3	122.9	110	0.09
P8	16	7.27	1308	1.7	13.4	199.5	193.4	408.1	72.3	116.7	0.00

P9	21	7.12	1222	1.7	8.3	137	192.3	333.1	114.7	117.4	0.00
P10	16	7.35	1315	1.6	14.6	174.8	189.1	396.4	132.7	117.4	0.00
River	-	n.d.	n.d.	4.3	8.2	n.d.	n.d.	249.9	n.d.	n.d.	n.d.

(n.d.: not determined)

Table S4: Isotopic results of field campaigns

Results of isotopic characterization of field campaigns samples

Sample	$\delta^{15}N_{NO3}$ (‰)	$\delta^{18}O_{NO3}$ (‰)	$\delta^{34}S_{SO4}$ (‰)	$\delta^{18}O_{SO4}$ (‰)	$\delta^{2}H_{H20}$ (‰)	$\delta^{18}O_{H20}$ (‰)	$\delta^{13}C$ (‰)
June 2013							
P1 (NGW)	+13.0	+2.8	+6.7	+9.8	-47.0	-8.2	-13.3
P2	+20.6	+6.8	+8.3	+10.5	-48.9	-8.4	-10.6
P3	n.d.	n.d.	+10.4	+10.8	-47.5	-8.4	n.d.
P5	n.d.	n.d.	+10.6	+9.4	-48.7	-8.3	-9.9
P8	+9.5	+4.7	+8.5	+11.1	-46.4	-7.1	-12.6
P9	+15.1	+9.5	+8.7	+10.7	-46.3	-7.6	-12.0
P10	+21.0	+4.5	+8.3	+10.7	-46.8	-8.6	-11.1
River	+12.1	+4.7	+8.6	+9.2	-48.5	-7.4	n.d.
September 2013							
P1 (NGW)	+17.5	+9.7	+8.3	+10.5	n.d.	n.d.	-12.4
P2	+26.7	+16.6	+8.5	+11.1	n.d.	n.d.	-12.3
P3	n.d.	n.d.	+10.0	+10.8	n.d.	n.d.	n.d.
P5	+17.0	+7.8	+10.0	+9.0	n.d.	n.d.	-13.8
P8	+15.7	+7.8	+9.1	+10.0	n.d.	n.d.	-13.3
P9	+17.9	+11.8	+9.8	+10.3	n.d.	n.d.	-12.7
P10	+19.9	+12.5	+9.3	+10.2	n.d.	n.d.	-12.9
River	+22.2	+13.4	+9.2	+10.3	n.d.	n.d.	n.d.
July 2014							
P1 (NGW)	+18.8	+11.4	n.d.	n.d.	-48.8	-8.2	-13.9
P2	+25.3	+16.10	n.d.	n.d.	-43.4	-6.9	-12.5
P3	n.d.	n.d.	n.d.	n.d.	-47.7	-8.0	n.d.
P5	+24.2	+10.6	n.d.	n.d.	-43.1	-6.9	-13.3
P8	+18.8	+13.0	n.d.	n.d.	-45.0	-7.2	-12.3
P9	n.d.	n.d.	n.d.	n.d.	-44.6	-7.2	-12.4
P10	+19.1	+10.9	n.d.	n.d.	-47.1	-7.6	-12.2
River	+24.8	+13.0	n.d.	n.d.	-51.1	-8.5	n.d.
March 2015							
P1 (NGW)	+13.9	+5.6	n.d.	n.d.	n.d.	n.d.	n.d.
P2	+17.3	+9.3	n.d.	n.d.	n.d.	n.d.	n.d.
P3	n.d.	n.d.	n.d.	n.d.	n.d.	n.d.	n.d.

P5	+14.5	+3.5	n.d.	n.d.	n.d.	n.d.	n.d.
P8	+12.6	+5.1	n.d.	n.d.	n.d.	n.d.	n.d.
P9	+15.0	+5.3	n.d.	n.d.	n.d.	n.d.	n.d.
P10	+14.3	+4.8	n.d.	n.d.	n.d.	n.d.	n.d.
River	+11.4	+4.7	n.d.	n.d.	n.d.	n.d.	n.d.

(n.d.: not determined; NGW: native groundwater)

Table S5: Nitrate concentration in Llobregat River

Results of nitrate concentrations of river samples.

Date		Sample	NO_3^- (mg/L)
June 2013	2013/06/18	River	6.1
	2013/06/18		6.0
	2013/06/18		6.2
	2013/06/18		5.8
July 2013	2013/07/11	River	17.4
Sept 2013	2013/09/05	River	8.4
July 2014	2014/07/22	River	10.09
	2014/07/22		4.96
	2014/07/23		6.25
	2014/07/23		4.49
March 2015	2015/03/01	River	8.2

Figure S1

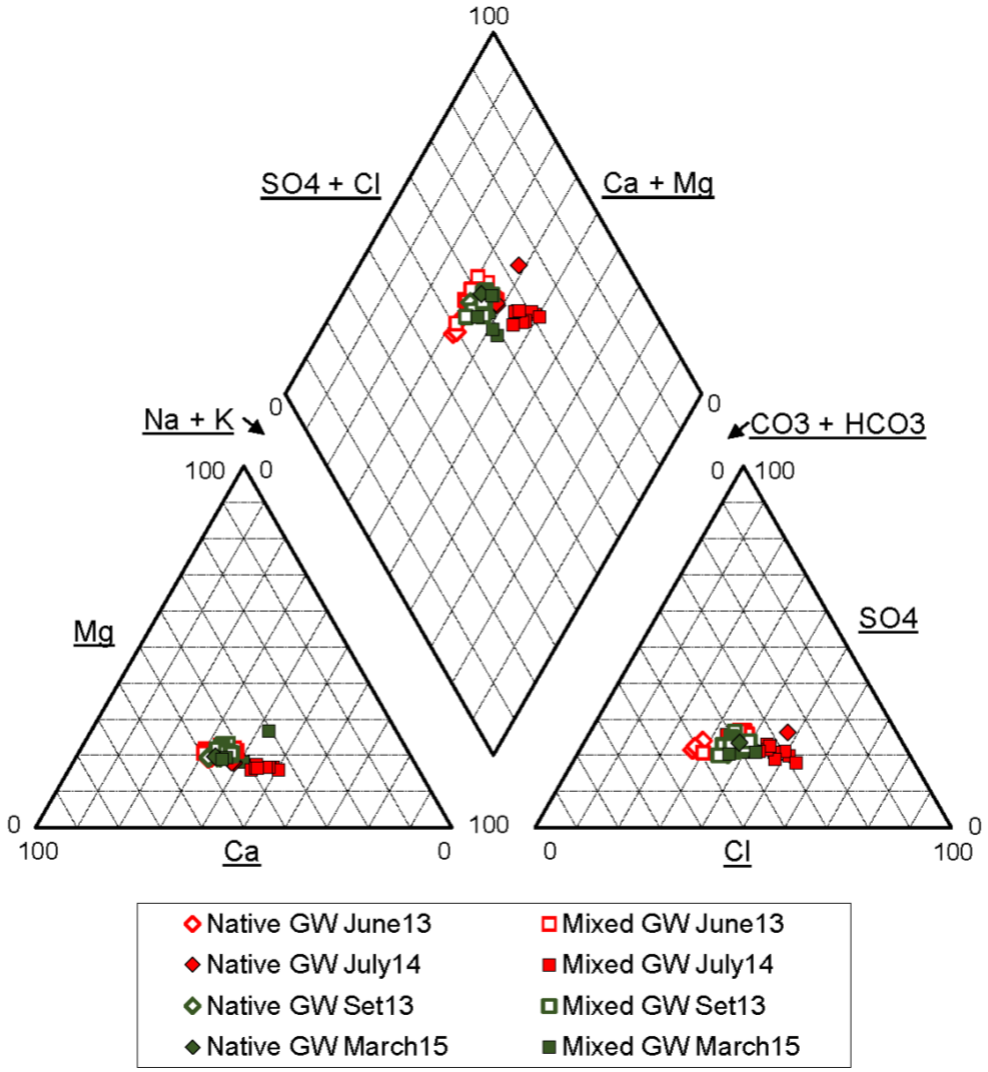

Figure S1. Piper diagram showing all the native (P1) and mixed (P2, P3, P5, P8, P9, P10) groundwater samples

Figure S2

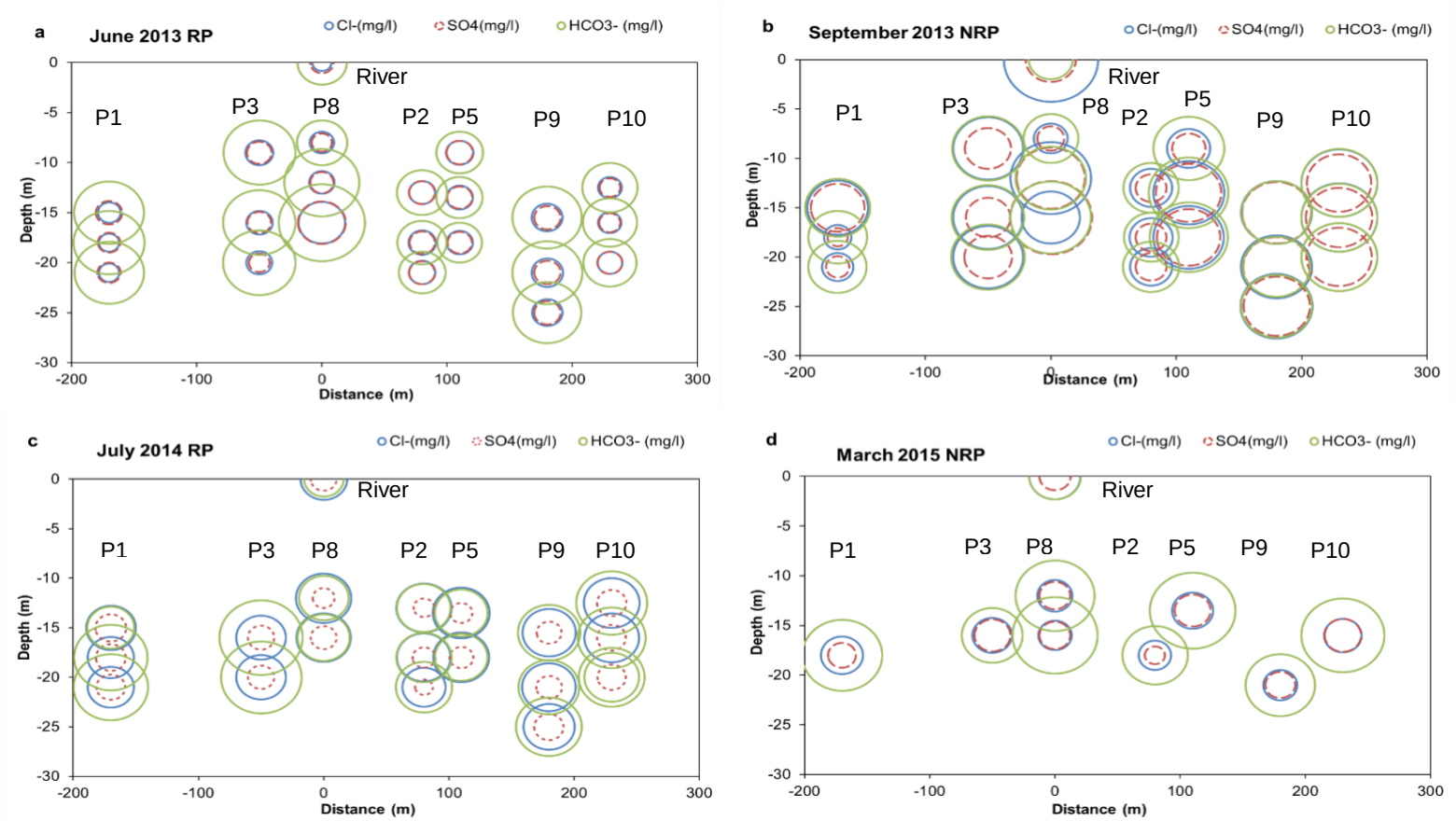

Figure S2. Changes in the concentration of major anions in depth-specific groundwater samples along the flow path during under both RPs (a, c) and NRPs (b, d). Values for the Llobregat river samples are also shown. The size of the symbols is proportional to the corresponding concentration value. Concentration ranged from 99.7 to 274.6 mg L^{-1} for Cl, from 103.3 to 231.4 mg L^{-1} for $SO4^{2-}$ and from 194 to 412.4 mg L^{-1} for HCO_3^-. Concentration values are given in Table S3.